

## Invited Research Papers

## The myth of the Messinian Dardanelles: Late Miocene stratigraphy and palaeogeography of the ancient Aegean-Black Sea gateway



Wout Krijgsman<sup>a</sup>, Marius Stoica<sup>b,\*</sup>, Thomas M. Hoyle<sup>a,c</sup>, Elisabeth L. Jorissen<sup>a</sup>, Sergei Lazarev<sup>a</sup>, Lea Rausch<sup>b,d</sup>, Diksha Bista<sup>e,f</sup>, Mehmet Cihat Alçiçek<sup>g</sup>, Ayhan Ilgar<sup>h</sup>, Lars W. van den Hoek Ostende<sup>i</sup>, Serdar Mayda<sup>j</sup>, Isabella Raffi<sup>k</sup>, Rachel Flecker<sup>e</sup>, Oleg Mandic<sup>l</sup>, Thomas A. Neubauer<sup>i,m</sup>, Frank P. Wesselingh<sup>a,i</sup>

<sup>a</sup> Department of Earth Sciences, Utrecht University, Budapestlaan 17, 3584 CD Utrecht, the Netherlands

<sup>b</sup> Department of Geology, Bucharest University, Bălcescu Bd. 1, Bucharest 010041, Romania

<sup>c</sup> CASP, West Building, Madingley Rise, Madingley Road, Cambridge CB3 0UD, UK

<sup>d</sup> Petrostrat, Tan-y-Graig, Parc Caer Seion, Conwy LL32 8FA, UK

<sup>e</sup> BRIDGE, School of Geographical Sciences and Cabot Institute, University of Bristol, University Road, Bristol BS8 1SS, UK

<sup>f</sup> NERC Isotope Geosciences Laboratory, British Geological Survey, Keyworth NG12 5GG, UK

<sup>g</sup> Pamukkale University, Department of Geology, 20070 Denizli, Turkey

<sup>h</sup> Department of Geological Research, General Directorate of Mineral Research and Exploration (MTA), 06800 Ankara, Turkey

<sup>i</sup> Naturalis Biodiversity Center, Darwinweg 2, 2333 CR Leiden, the Netherlands

<sup>j</sup> Faculty of Science, Biology Department, Ege University, Bornova, Izmir, Turkey

<sup>k</sup> Dipartimento di Ingegneria e Geologia (InGeo), Università degli Studi "G. d'Annunzio" di Chieti-Pescara, Chieti Scalo, Italy

<sup>l</sup> Geological-Palaeontological Department, Natural History Museum Vienna, Burgring 7, Vienna 1010, Austria

<sup>m</sup> Department of Animal Ecology and Systematics, Justus Liebig University, Heinrich-Buff-Ring 26-32 IFZ, 35392 Giessen, Germany

## ARTICLE INFO

## Keywords:

Miocene

Turkey

Paratethys

Stratigraphy

Paleontology

North Anatolian Fault

## ABSTRACT

The Dardanelles region has formed a key gateway connecting the Eastern Paratethys and the Aegean/Mediterranean since the late Miocene. Its sedimentary sequences contain crucial information about connectivity and tectonics but so far lack unambiguous age constraints. Only a few Miocene marine episodes have been documented and fossil assemblages are predominantly composed of Paratethyan fauna (mollusks and ostracods). Here, we apply an integrated stratigraphic approach and use the recently established chronostratigraphy for the Eastern Paratethys to re-evaluate the faunal assemblages and palaeoenvironments of the Seddülbağ and İtepe sections that allegedly played a crucial role in the geodynamic evolution of the Dardanelles during the Messinian-Zanclean. The Paratethyan ostracods and mollusks, however, clearly indicate that these sections correspond to the middle Tortonian (~9 Ma; Bessarabian-Khersonian in Eastern Paratethys terminology). Nannofossil assemblages are dominated by a mixing of reworked taxa from the late Eocene and Oligocene and no age-diagnostic taxa have been observed. Dinoflagellate analyses are also hampered by reworking and mainly reveal non-marine (fresh to oligohaline) aquatic conditions. Fossil mammal remains in the Seddülbağ section and other localities in the region confirm the late Miocene age. Strontium (<sup>87</sup>Sr/<sup>86</sup>Sr) isotope ratios of the anomalohaline (brackish) ostracods are significantly below open ocean values and similar to values obtained from Khersonian ostracods of Bulgaria. Fresh water assemblages reveal much higher <sup>87</sup>Sr/<sup>86</sup>Sr values, which are interpreted to reflect the composition of local rivers. We conclude that in late Miocene times the Dardanelles region was a fresh to anomalohaline embayment, ephemerally connected to the Eastern Paratethys. We found no evidence for a major Messinian erosional surface nor for marine Mediterranean fossils indicative of the early Zanclean. Our results furthermore indicate that the proposed Messinian age for the propagation of the North Anatolian Fault into the Dardanelles region must be revised.

\* Corresponding author.

E-mail addresses: [W.Krijgsman@uu.nl](mailto:W.Krijgsman@uu.nl) (W. Krijgsman), [marius.stoica@unibuc.ro](mailto:marius.stoica@unibuc.ro) (M. Stoica), [thomas.hoyle@casp.org.uk](mailto:thomas.hoyle@casp.org.uk) (T.M. Hoyle), [E.L.Jorissen@uu.nl](mailto:E.L.Jorissen@uu.nl) (E.L. Jorissen), [S.Lazarev@uu.nl](mailto:S.Lazarev@uu.nl) (S. Lazarev), [diksha.bista@bristol.ac.uk](mailto:diksha.bista@bristol.ac.uk) (D. Bista), [alcicek@pau.edu.tr](mailto:alcicek@pau.edu.tr) (M.C. Alçiçek), [lars.vandenhoekestende@naturalis.nl](mailto:lars.vandenhoekestende@naturalis.nl) (L.W. van den Hoek Ostende), [serdar.mayda@ege.edu.tr](mailto:serdar.mayda@ege.edu.tr) (S. Mayda), [isabella.raffi@unich.it](mailto:isabella.raffi@unich.it) (I. Raffi), [R.Flecker@bristol.ac.uk](mailto:R.Flecker@bristol.ac.uk) (R. Flecker), [oleg.mandic@nhm-wien.ac.at](mailto:oleg.mandic@nhm-wien.ac.at) (O. Mandic), [Thomas.A.Neubauer@allzool.bio.uni-giessen.de](mailto:Thomas.A.Neubauer@allzool.bio.uni-giessen.de) (T.A. Neubauer), [frank.wesselingh@naturalis.nl](mailto:frank.wesselingh@naturalis.nl) (F.P. Wesselingh).

<https://doi.org/10.1016/j.palaeo.2020.110033>

Received 13 July 2020; Received in revised form 16 September 2020; Accepted 16 September 2020

Available online 22 September 2020

0031-0182/ © 2020 Elsevier B.V. All rights reserved.

## 1. Introduction

The present-day Black Sea is connected via the Bosphorus Strait, the Sea of Marmara, the Dardanelles Strait and the Aegean Sea to the Mediterranean (Fig. 1). Based on the sedimentary successions in the Sea of Marmara, the modern Dardanelles Strait is thought to have originated in the middle-late Pleistocene (Erol, 1992; Ergun and Ozel, 1995; Parke et al., 1999; Okay et al., 2000; Imren et al., 2001; Le Pichon et al., 2001; Gökaşan et al., 2008, 2012). The Bosphorus Strait possibly developed only in the late Pleistocene (Gökaşan et al., 1997; Algan et al., 2001), and middle Pleistocene connections between the Marmara Sea and Black Sea Basin may have run through an İznik or a Sapanca corridor (IS in Fig. 1: İslamoğlu, 2009; Le Pichon et al., 2016; Krijgsman et al., 2019).

The late Miocene Paratethys Sea, the unified precursor of the Black Sea-Caspian Sea, was also connected to the Mediterranean-Aegean Basin through a shallow marine gateway, as evidenced by the presence of late Miocene Paratethyan faunas in sections in northern Greece and western Turkey (Erguvanli, 1955; Gramann and Kockel, 1969; Erdoğan, 1978; Sümengen et al., 1987; Stevanovic et al., 1989; Rögl et al., 1991; Görür et al., 1997; Çağatay et al., 1998, 2006; Syrides, 1998; Popov and Nevesskaya, 2000; Popov et al., 2006) and Mediterranean fauna in sections in Romania and Russia (Krijgsman et al., 2010; Radionova et al., 2012; Stoica et al., 2013; Golovina et al., 2019; Lazarev et al., 2020). The exact position of this Miocene gateway is still uncertain (Van Baak et al., 2016b; Karakitsios et al., 2017); one option being a gateway through the Balkans (BG in Fig. 1: Stevanovic et al., 1989; Suc et al., 2015), the alternative an ancient Bosphorus/Marmara/Dardanelles connection (BMD in Fig. 1: Lüttig and Steffens, 1976; Görür et al., 2000; Popov et al., 2006).

The oldest Paratethyan fauna in the Aegean region is attributed to the middle Miocene (Umut et al., 1983). Late Miocene Paratethyan mollusk and ostracod assemblages are more widespread (Gramann and Kockel, 1969; Rögl et al., 1991; Popov and Nevesskaya, 2000) and have been observed as far south as the Denizli Basin in southwestern Turkey (Stevanovic et al., 1989; Wesselingh et al., 2008; Lazarev, 2020; Rausch et al., 2020). The mollusk fauna in the Denizli Basin is dominated by endemic species, and several of the mollusk taxa are the oldest records of modern “Pontocaspian” lineages. These Pontocaspian nowadays form an isolated brackish (anomalous) fauna living in the Caspian Sea, Aral Sea and the estuarine regions of the Black Sea (Alçiçek et al., 2015; Wesselingh et al., 2019). The exact migration time and pathway of these particular species to southwestern Turkey remains a mystery (Lazarev, 2020; Rausch et al., 2020), but their ancestors most likely originated in the Paratethys and passed through the Aegean domain, and potentially via an ancient Dardanelles Strait. The palaeogeographic evolution of the Dardanelles is thus fundamental to explain the biogeographic evolution of the entire region.

The Neogene deposits of the Dardanelles region (Fig. 2) comprise thick sedimentary successions (Kirazlı and Alçıtepe formations) that contain abundant micro- and macrofauna of Paratethyan origin (Ternek, 1949; Erguvanli, 1955; Erdoğan, 1978; Umut et al., 1983; Sümengen et al., 1987; Çağatay et al., 1998, 2006). This fauna suggests that the Miocene Dardanelles region was fully connected to the former Black Sea domain and episodically formed a southern embayment of the Paratethys Sea (Lüttig and Steffens, 1976). The oldest Neogene sediments in the Dardanelles region are continental-lacustrine deposits, dated by mammal biostratigraphy to correspond to the Serravallian (Ünay and De Bruijn, 1984). The rich Paratethyan fauna of the overlying Kirazlı and Alçıtepe formations are generally attributed to the late

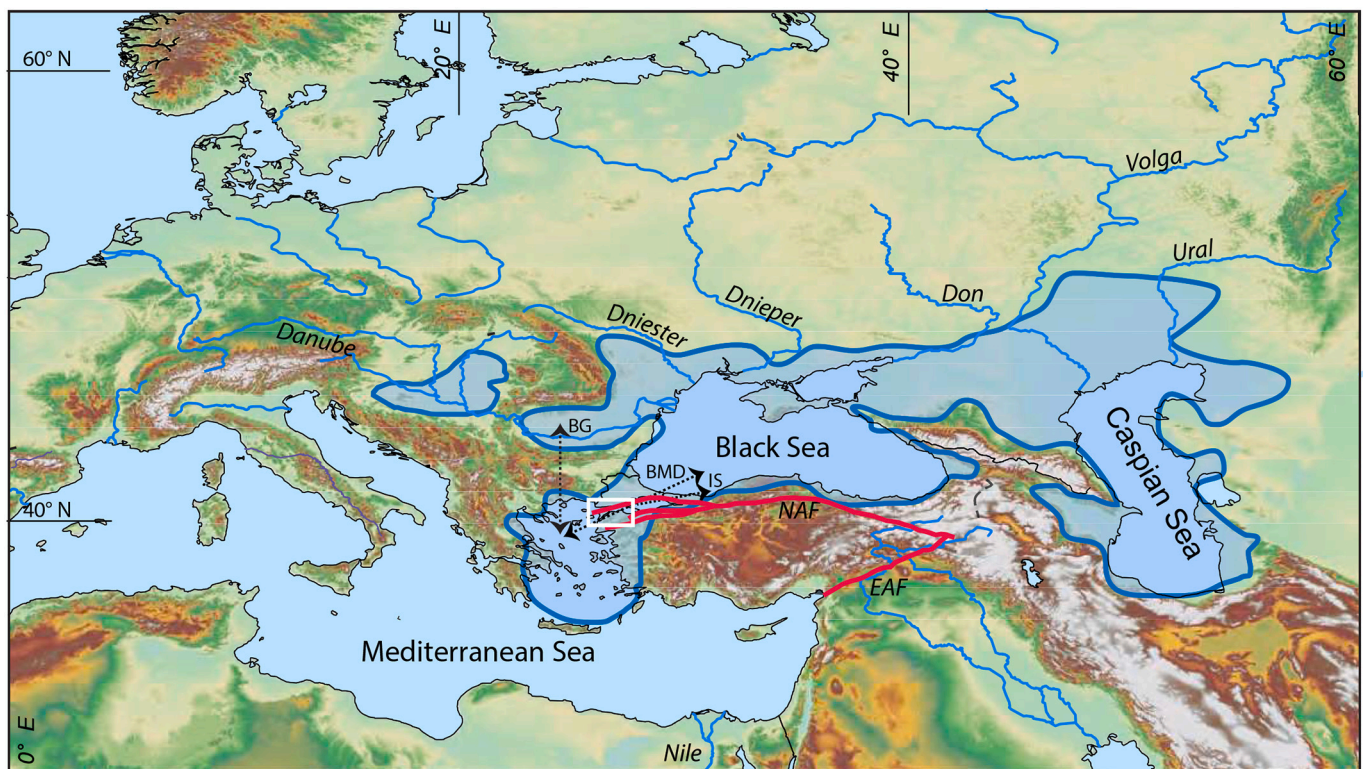


Fig. 1. Elevation map showing the extent of the late Miocene Black and Caspian Sea and their drainage basins, modified after Grothe et al. (2020). The former Paratethys Sea during the latest Miocene is outlined according to Popov et al. (2006) who considered the Aegean domain as an intermittent region between Mediterranean and Paratethys. White rectangle denotes the study area of the Dardanelles. Red lines denote the North Anatolian Fault (NAF) Zone that runs through the Dardanelles region and the East Anatolian Fault (EAF). Black lines with arrows indicate the hypothetical gateways between Aegean and Paratethys: BG - Balkan Gateway (Stevanovic et al., 1989; Suc et al., 2015), BMD - Bosphorus/Marmara/Dardanelles connection (Lüttig and Steffens, 1976; Görür et al., 2000; Popov et al., 2006), IS - İznik/Sapanca corridor (İslamoğlu, 2009; Le Pichon et al., 2016). (For interpretation of the references to colour in this figure legend, the reader is referred to the web version of this article.)



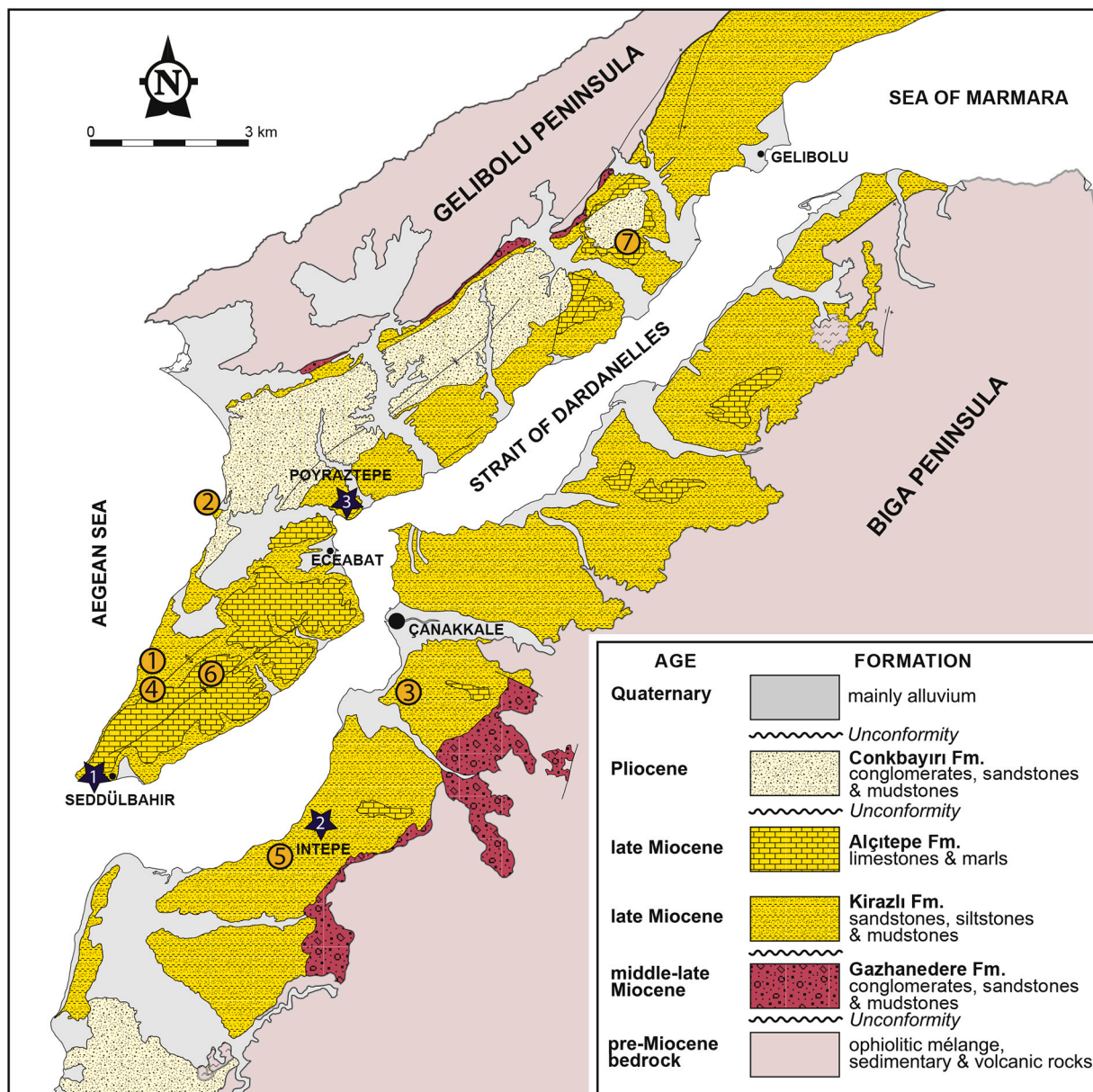


Fig. 2. Geological map of the Dardanelles region. Black stars indicate the studied sections; 1) Seddülbağır, 2) İntepe-2 and 3) Poyraztepe. Circles denote fossil mammal localities from literature; 1) Nebisuyu, 2) Kabatepe, 3) Bayraktepe-1 and -2, 4) Sığındere; 5) Erenköy, 6) Değirmendere and 7) Bayırköy (see Suppl. Material for details).

Miocene; Tortonian-Messinian in Mediterranean terms and Pannonian/Bessarabian-Pontian in Paratethys nomenclature (see Şentürk and Karaköse, 1987; Sümengen et al., 1987; Çağatay et al., 2006). Absolute age control of the formation is rare and restricted to radio-isotopic dating of an intercalated basalt unit at the basal part, providing ages of  $10.1 \pm 0.2$  and  $9.5 \pm 0.3$  Ma (Ercan et al., 1995). This age is in agreement with the assumed late Miocene age of the overlying *Chersonimactra*-bearing sediments of the Alçıtepe Fm (Şentürk and Karaköse, 1987).

In a mainly tectonic study, Armijo et al. (1999) neglected all the faunal evidence and placed the Alçıtepe Formation in the early Pliocene ( $< 5.33$  Ma), because they correlated an unconformity below the formation to be the Messinian Erosional Surface (MES). This Pliocene age had far-reaching consequences for regional tectonics as it was used to date the propagation of the North Anatolian Fault into the Dardanelles region (Fig. 1). This correlation was generally rejected by other geologists (e.g., Yaltırak et al., 2000; Okay et al., 2004; Rangin et al., 2004;

Şengör et al., 2005; Zattin et al., 2005). Recently, the debate revived again by the documentation of the MES in the Seddülbağır and İntepe sections, supported this time by the presence of Pliocene nannofossils in the Alçıtepe Fm (Melinte-Dobrinescu et al., 2009). The presence of these Atlantic nannofossils led to the hypothesis that the Alçıtepe deposits correspond to the marine Zanclean flooding (Karakaş et al., 2018), when Atlantic waters cascaded into the largely desiccated Mediterranean basin at the end of the Messinian Salinity Crisis (5.33 Ma). It has, however, been shown that these nannofossils are not always reliable markers in Mediterranean and Paratethyan environments (Di Stefano and Sturiale, 2010; Van Baak et al., 2016a, 2017; Stoica et al., 2018; Golovina et al., 2019). In addition, it remains very difficult to reconcile a Pliocene marine flooding and Miocene lacustrine-anomalous endemic Paratethyan faunal assemblages in the Alçıtepe Formation.

Accurate age correlations within the Paratethys domain have long been hampered by the absence of a reliable geological time scale for the

region. In the last two decades, numerous studies focused on the integration of biostratigraphy, magnetostratigraphy and Ar-Ar dating in the Paratethys domain and have provided coherent correlations to the standard GTS, especially dating the late Miocene evolutionary development of mollusks and ostracods (Stoica et al., 2007, 2013, 2016; Krijgsman et al., 2010; Vasiliev et al., 2011; ter Borgh et al., 2013; Van Baak et al., 2015, 2016b; Palcu et al., 2019a; Lazarev et al., 2020). With this updated chronologic framework for the Paratethys now available, we are confident that we are able to improve the age estimates of faunal elements in the enigmatic Alçıtepe Formation of the Dardanelles region through an integrated stratigraphic study.

For this purpose, we logged and studied in detail the Seddülbahir section on the southern tip of the Gelibolu Peninsula and the İntepe region on the eastern shore near Çanakkale (Fig. 2). Both play a crucial role in the age debate on the presence or absence of Messinian-Zanclean deposits in the region (Sümengen et al., 1987; Melinte-Dobrinescu et al., 2009). According to the most recent publications, the Seddülbahir section comprises the MES at its base and contains evidence of marine Zanclean fauna in the main outcrop (Melinte-Dobrinescu et al., 2009; Karakaş et al., 2018). The Paratethyan fossils of the same section, however, indicate a much older (Tortonian-Messinian) age (Erguvanli, 1955; Erdoğan, 1978; Sümengen et al., 1987; Çağatay et al., 2006). Here, we describe the sedimentary facies distribution, analyse ostracods and mollusks, re-evaluate the nannofossil results, study the palynology, check for mammal remains and determine the strontium isotope ratios

of the ostracods to differentiate between marine Pliocene and anomalohaline Miocene Paratethys environments.

## 2. Regional stratigraphic framework

The key sedimentary successions of Miocene deposits in the Dardanelles region are well-exposed in the Gelibolu and Biga peninsulas and consist of the middle-upper Miocene Gazhanedere, Kırızlı and Alçıtepe formations (Fig. 2). The succession is overlain in the Dardanelles region by Plio-Pleistocene alluvial deposits of the Conkbayırı Formation. Two different views on the regional stratigraphic framework exist (Fig. 3). The conventional view describes only conformable contacts and lateral transitions of three Miocene formations (e.g., Sümengen et al., 1987; Sakinç et al., 1999; Çağatay et al., 2006). In Fig. 3, the Kırızlı-Alçıtepe transition is tentatively placed in the lower Messinian, but it should be noted that absolute age control on these formations is very poor. An alternative view has strong tilting of the Gazhanedere and Kırızlı formations and the Alçıtepe Formation filling in a strongly erosional relief, which is hypothesised to be the MES (Armijo et al., 1999; Melinte-Dobrinescu et al., 2009). As a result, these authors consider the Alçıtepe Fm as Zanclean. Here, we describe the main stratigraphic and sedimentological characteristics of the three key formations of the present section, where we follow the regional stratigraphic framework of Çağatay et al. (2006).

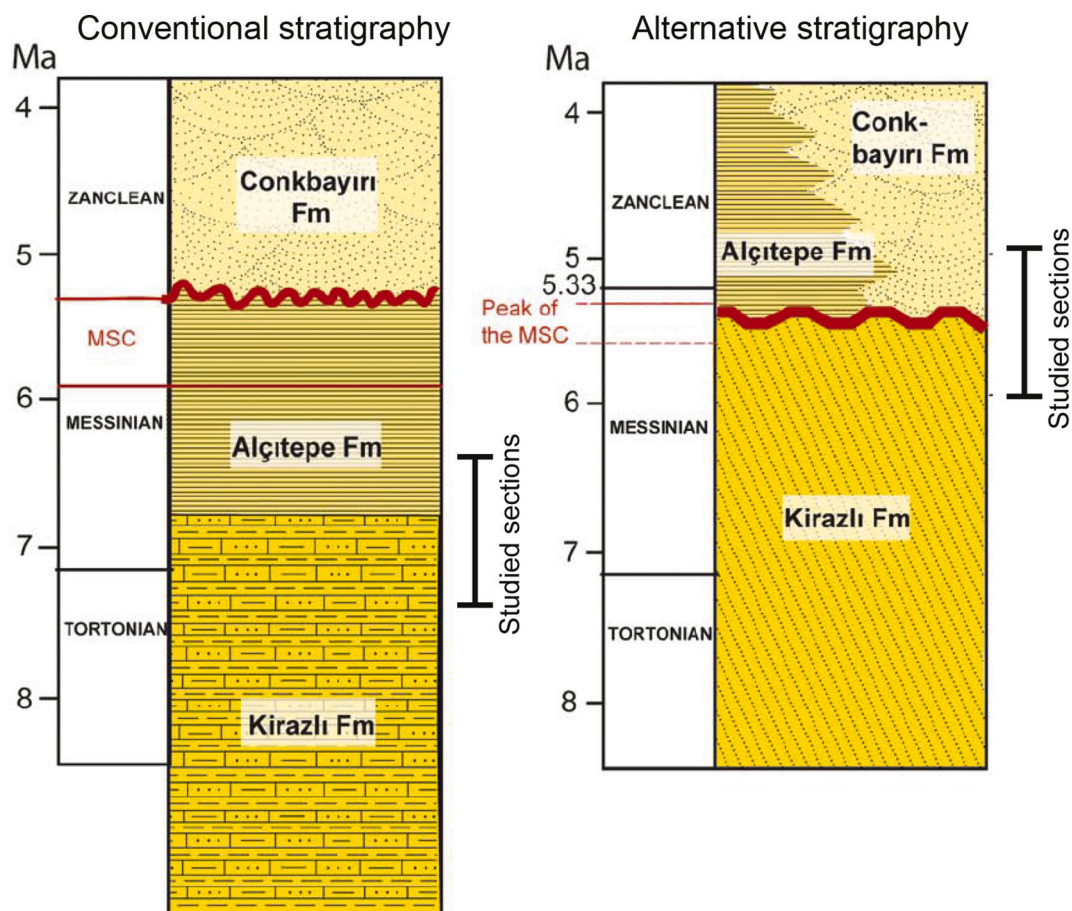


Fig. 3. Two different views on the regional stratigraphy of the Dardanelles region (after Melinte-Dobrinescu et al. (2009)). A) Conventional stratigraphic scheme showing conformable contacts between the Kirazlı and Alçıtepe formations that are both considered to be of late Miocene age (Sakinç et al., 1999; Sakinç and Yaltırak, 2005) and B) alternative stratigraphic scheme (Armijo et al., 1999; Melinte-Dobrinescu et al., 2009) showing a major angular unconformity between the Kirazlı and Alçıtepe formations, and the latter formation attributed to the Zanclean. Key problem here is that no robust age constraints are available for the two formations and that it is not clear how much time is missing below the unconformity. We note that the Kirazlı-Alçıtepe transition in the conventional scheme is tentatively placed in the lower Messinian, but there are many indications that this boundary is significantly older (see arguments in this paper). The stratigraphic interval of our studied sections is schematically shown next to both schemes.



## 2.1. Gazhanedere Formation

The Gazhanedere Formation unconformably overlies the pre-Miocene bedrock of the Dardanelles and consists of reddish-brownish conglomerates, sandstones and mudstones. The mainly coarse-grained facies association is composed of multistore fluvial palaeo-channels representing the deposits of a stream-dominated alluvial fan. The mammal fauna indicates a late Astaracian-Vallesian age (~11 Ma;

Hilgen et al., 2012) for the Gazhanedere Formation (Kaya, 1982, 1989).

## 2.2. Kirazlı Formation

The siliciclastic deposits of the Kirazlı Formation extend over large areas across the Dardanelles Strait between Marmara and the Aegean Sea (Fig. 2). This formation unconformably overlies the Eocene-Oligocene volcanic and sedimentary rocks and the middle-upper Miocene

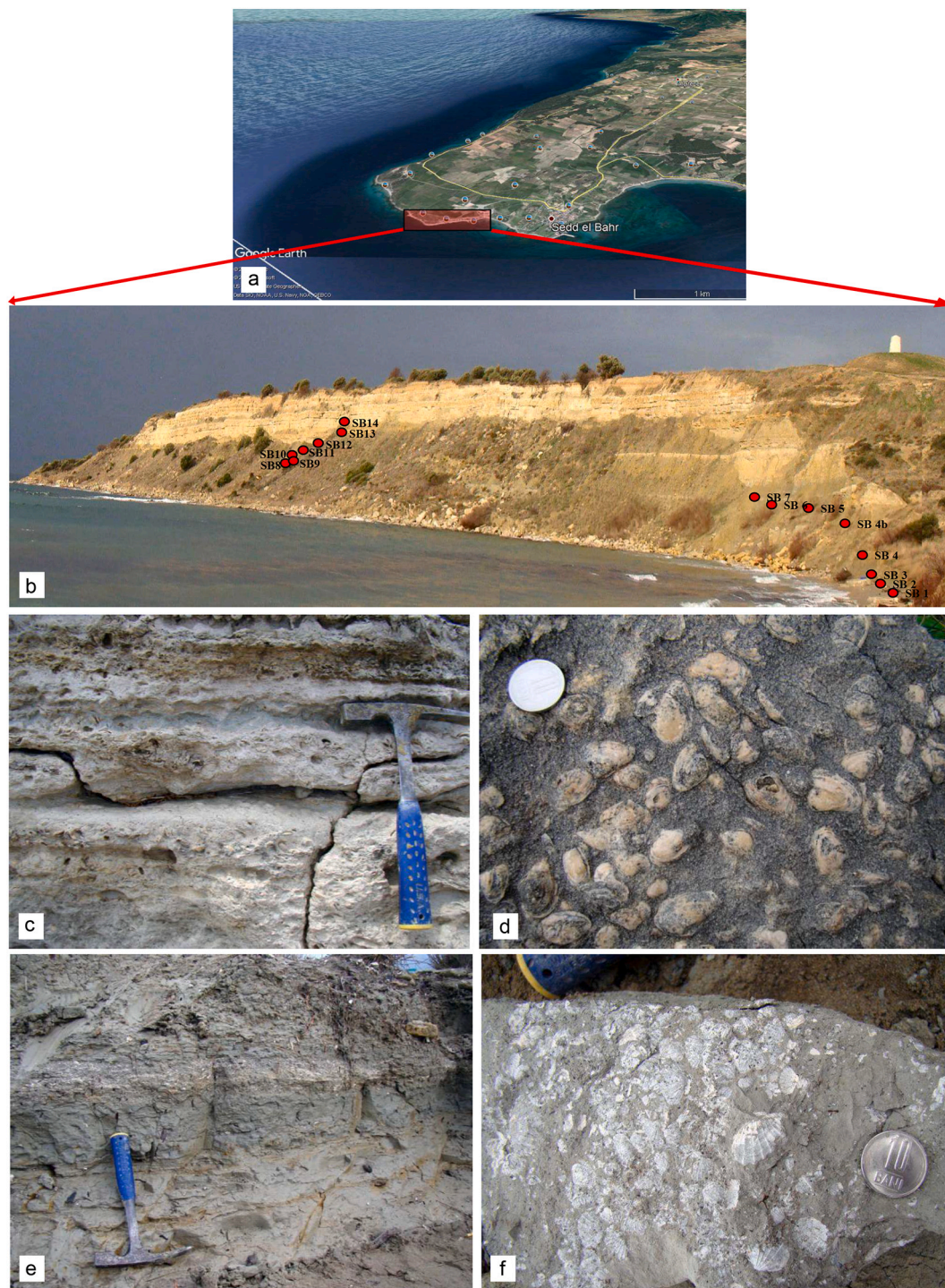


**Fig. 4.** a) The location of Seddülbahir section on the southern tip of the Gelibolu Peninsula (Map data: Google, Maxar Technologies); b) Photo of the Seddülbahir section (west) where the upper Miocene (upper Bessarabian-Khersonian) sediments are exposed. (micropalaeontological sample levels are marked by red dots); c), d) Calcareous sandstones rich in *Chersonimactra bulgarica* shells (0.7 m level); e), f) Grey clay rich in *Plicatiformes* cf. *plicatofittoni* (0.2 m level). (For interpretation of the references to colour in this figure legend, the reader is referred to the web version of this article.)



alluvial Gazhanedere Formation. The Kirazlı Formation is both laterally and vertically transitional with the overlying Alçıtepe Formation. The successions are generally continuous and no intraformational unconformities, indicating interruption of sedimentation, are observed.

The Kirazlı Formation is composed of sandstones, granule to fine pebble conglomerates, siltstones and mudstones. Within the sandstones planar parallel stratification, wave-ripple cross-lamination, planar-, trough- and hummocky cross-stratification are found. The mudstones are interlayered with thin, sheet-like beds of siltstones and sandstones showing planar parallel stratification, wave-ripple cross-lamination. Conglomerates are mainly planar parallel stratified or low-angle cross stratified. The Kirazlı Formation consists of six facies associations, viz. i) nearshore heterolithic mudstone-sandstone deposits, ii) wave-worked shoreface sandstones, iii) gravelly foreshore, iv) sandy-gravelly shoal-water delta deposits, v) lagoonal mudstones and vi) backshore sandstones. The vertical stacking pattern of the Seddülbahir and İntepe sections show that facies associations alternate several times which indicates relative base level changes during deposition.

### 2.3. Alçıtepe Formation

The carbonate rocks of the Alçıtepe Formation crop out in relatively

small areas, on both the Gelibolu and Biga peninsulas. The Alçıtepe Formation is laterally transitional and vertically overlies the siliciclastic deposits of the Kirazlı Formation. Well-preserved outcrops are found at the Seddülbahir and İntepe localities (Fig. 2).

The Alçıtepe Formation consists mainly of fossiliferous limestones, oolites, calcarenites, stromatolitic limestones, marls and siltstones. It is generally very rich in fossils. The thin-bedded fossiliferous limestones, oolites, calcarenites are laterally extensive and mainly tabular. Oolite beds are planar parallel or planar cross-stratified. Stromatolites occur as domes, in subspherical or columnar forms. They commonly overlie planar or undulated-bedded siltstones. The accommodations between the stromatolite growth forms are filled by intraclasts, ooids, pisoliths, carbonate sands and shell fragments.

### 3. Methods

We analyzed two sections in the Dardanelles region for this study; Seddülbahir and İntepe-2 (Sections 9 and 10 of Melinte-Dobrinescu et al., 2009). The Seddülbahir section (40°02'39"N; 26°10'53"E), located at the southernmost tip of the Gelibolu peninsula, is a well-exposed coastal cliff (Fig. 4). The section contains the Kirazlı-Alçıtepe transition according to Çağatay et al. (2006) and has entirely been

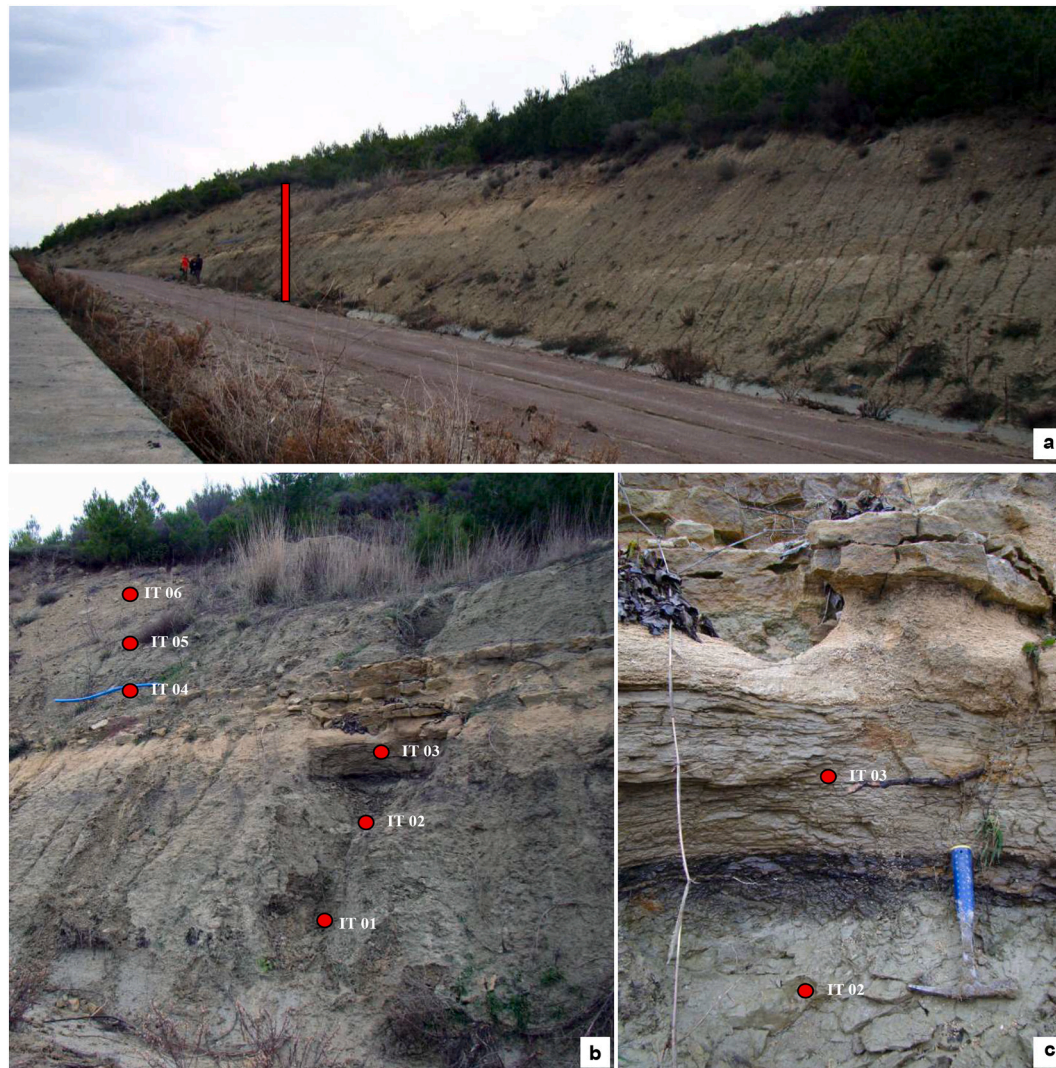


**Fig. 5.** a) Photo of the İntepe-2 section where the upper Miocene sediments are exposed (the red line marks the sampled section) b) The İntepe-2 with the position of micropalaeontological sample marked by dots; c) Detail of the lignite level that is overlain by silts with fresh water fauna and calcareous sandstones rich in anomalohaline *Chersonimactra* shells. (For interpretation of the references to colour in this figure legend, the reader is referred to the web version of this article.)



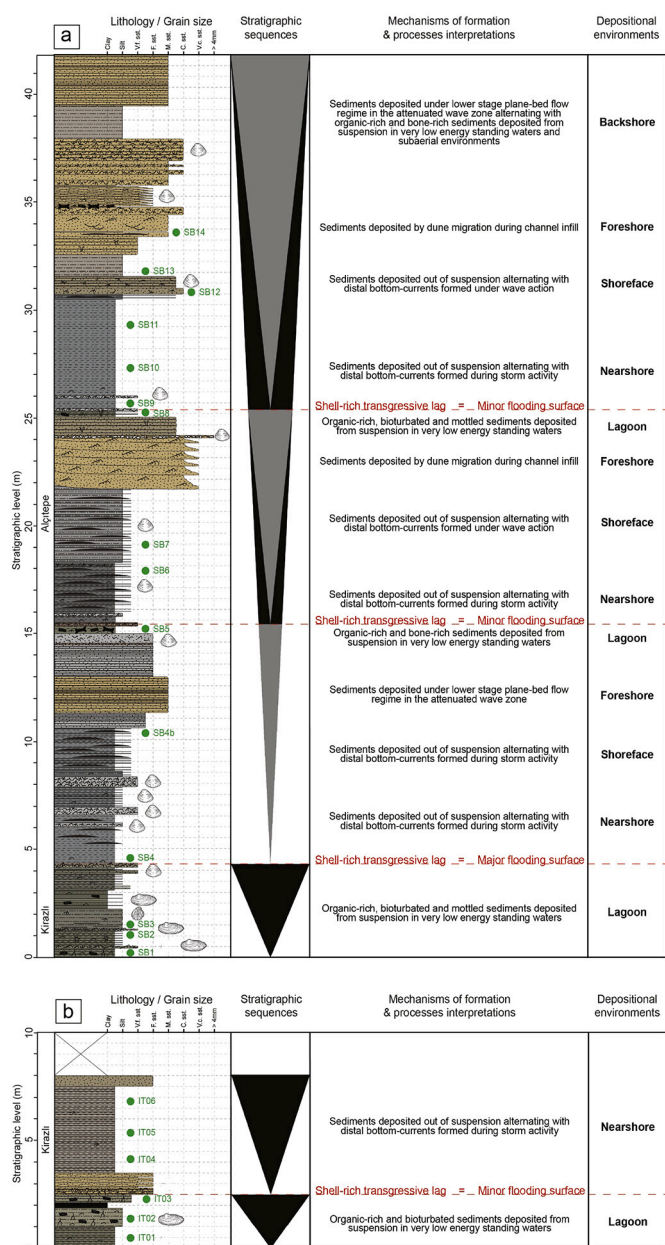


Fig. 6. Detailed sedimentological log of: a) the Seddülbahir section and b) the İntepe-2 section. For biostratigraphic data see legend to Fig. 7.

attributed to the Alçıtepe Formation by Melinte-Dobrinescu et al. (2009). The 41.5 m long section was logged at dm-scale for sedimentology and studied at m-scale for integrated stratigraphy.

The İntepe region is nowadays significantly disturbed by the construction of a new highway. We traced the characteristic coal bed, which Melinte-Dobrinescu et al. (2009) correlated to the MES, laterally in a ~ 10 m thick exposure (İntepe-2, Fig. 5) along a local road (40°01'40"N; 26°20'44"E). According to the regional stratigraphy, the İntepe section is slightly older than the Seddülbahir section and belongs entirely to the Kirazlı Formation following Çağatay et al. (2006). In the alternative scenario of Melinte-Dobrinescu et al. (2009), however, the Kirazlı-Alçıtepe boundary is placed at the coal bed of İntepe, which these authors assume to correspond to a 200 kyr hiatus, but without any visible unconformity. We logged and sampled the İntepe-2 section for sedimentologic and biostratigraphic analyses.

A total of 20 levels, 14 levels from the Seddülbahir and 6 from the İntepe-2 section, were analyzed for ostracods, with special focus on the

clay and silty intercalations. Samples were processed following standard methods (Stoica et al., 2013), sieved over 63 µm and handpicked under a Zeiss GSZ microscope. The preservation of ostracod shells is relatively good, especially for samples that come from the basal part of the Seddülbahir section. Ostracods were photographed with a ZEISS-Stemi SV11 microscope mounted with a NIKON digital camera.

Mollusk specimens were checked in the field at sections Seddülbahir and İntepe-2 and selected specimens were obtained for detailed taxonomic observations. One additional mollusk level was sampled in the Poyraztepe section (Section 5 of Melinte-Dobrinescu et al., 2009). Macro-photographs were made with a Leica M165 C stereomicroscope with attached DFC420 camera, using the focus stacking function of the Leica Application Suite software v. 4.4.0.

A total of 19 samples, twelve from Seddülbahir and seven from İntepe-2, were processed for analysis of the calcareous nannofossil assemblages. The samples were obtained in the same interval where Melinte-Dobrinescu et al. (2009) claimed to have found the lowermost Pliocene marker *Ceratolithus acutus*. 19 smear-slides were prepared using standard techniques and observed in the light microscope at a magnification of ca. 1200x.

Six samples, four from Seddülbahir (SB2, SB4, SB4B, SB11) and two from İntepe-2 (IT5 and IT lignite), were processed for palynological analysis using cold HCl (30%) to remove carbonates and cold HF (38%) to dissolve silicates. Samples were subjected to five minutes in an ultrasonic bath and sieved through meshes (125 and 10 µm) and the 10–125 µm fraction was retrieved. The residues were then mounted on slides using a light-curing adhesive and a cover slip added before curing the residue using a UV lamp. Slides were scanned for palynomorphs that could be identified in order to give an indication of depositional palaeoenvironments.

Seven samples were processed for strontium analyses; two samples from the Seddülbahir section (SB1 and SB10), three samples from the İntepe-2 section (IT1, IT3 and IT 6), and two samples from the Zelenka section, a Khersonian reference section located at the Bulgarian margin of the Eastern Paratethys (43°23'05"N; 28°25'56"E). Sr isotopic analysis was carried out on 3–5 well-preserved smooth-shelled ostracods. The isotopic measurements were carried out using a Thermo-Finnegan Triton thermal ionization mass spectrometer (TIMS) at the University of Bristol. Instrument performance was monitored using the NBS987 Sr standard, which produced an average of  $0.710248 \pm 0.00001$  (2 SD,  $n = 6$ ). Procedural Sr blank is negligible based on replicate measurement of NBS987 Sr with the batch of column chromatography ( $0.710247 \pm 0.00001$ ,  $n = 2$ ).

In the Seddülbahir section, a level with land snails (SB5, 15 m) was studied for fossil mammal analyses. A test sample was washed and sieved at the Natural History Museum of Ege University (İzmir) and Pamukkale University (Denizli), and further analyzed at the Naturalis Biodiversity Center in Leiden, the Netherlands. The material was measured using a Leica MZ16A with associated software and SEM photographs.

#### 4. Sedimentology

A detailed sedimentary log was drawn along the 41.5 m long Seddülbahir section (Fig. 6a). The lower part of the section (0–4.5 m) is mainly composed of greenish-grey claystones to siltstones with mm-thick planar silt laminations (Fig. 4e). These fine-grained sediments contain common-abundant mm-scale terrestrial organic material fragments, cm-scale vertical roots and shell fragments of freshwater-oligohaline mollusks (Fig. 4d, f). Also, dm- to m-scale very fine-grained light greenish-grey sandstone layers with cm-scale cross-stratifications occur that contain abundant shell fragments. Overall, this lower interval typically demonstrates organic-rich fine sediments that are heavily bioturbated and mottled. Sediments represent suspension deposition in very low energy settings such as a lagoonal environment. The lower part of the section is overlain by a shell-rich lag. This light greenish-

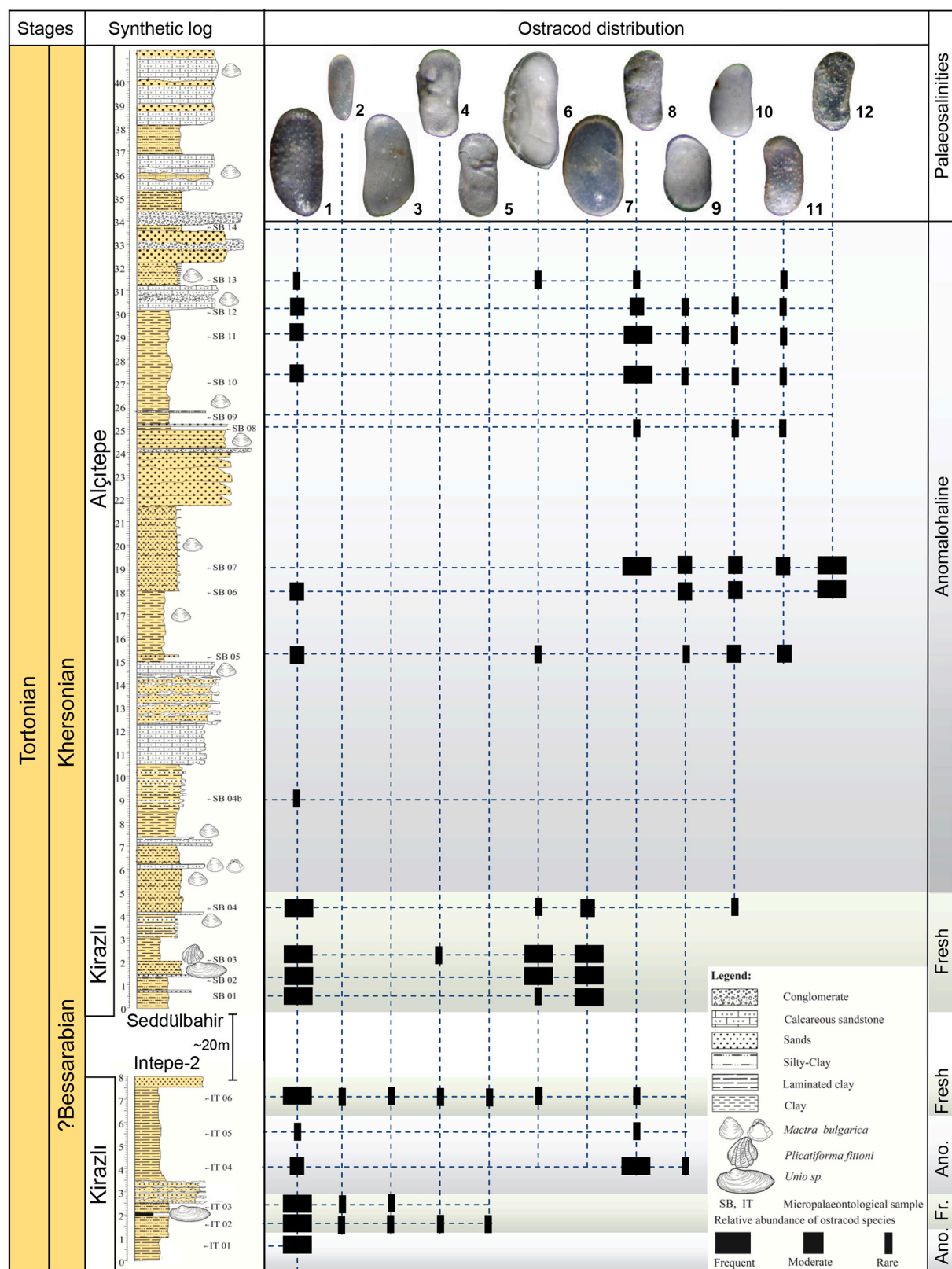


**Fig. 7.** Late Miocene ostracod occurrences in the Seddülbahir and İntepe-2 sections: 1. *Cyprideis torosa* (Jones); 2. *Darwinula stevensoni* (Brady & Robertson); 3. *Candona neglecta* Sars; 4. *Ilyocypris bradyi* Sars; 5. *Limnocythere levisreticulata* Stancheva; 6. *Candona angulata* Müller; 7. *Heterocypris formalis* (Mandelstam); 8. *Euxinocythere (E.) immutata immutata* Stancheva; 9. *Loxoconcha rimopora* Suzin; 10. *Xestoleberis fuscata* Schneider; 11. *Euxinocythere (E.) topolensis* Stancheva; 12. *Euxinocythere (E.) immutata bononiensis* Stancheva;





(caption on next page)

**Fig. 8.** a: The most representative ostracods from Seddülbahir and İntepe sections (late Miocene, late Bessarabian–Khersonian) (LV = left valve, RV = right valve, C = carapace, ♀ = female, ♂ = male). 1–3. *Candona angulata* Müller; 1. LV, external view; 2. C, view from RV; 3. C, ventral view. 4,5. *Candona neglecta* Sars; 5. LV, external view; 6. RV, external view. 6–8. *Heterocypris formalis* (Mandelstam); 6. LV, external view; 7. C, view from RV; 8. C, ventral view. 9–11. *Stanchevia* sp.; 9. LV, external view; 10, 11. RV, external view. 12, 13. *Ilyocypris bradyi* Sars; 12. LV, external view; 13. view from RV; 14–17. *Limnocythere levisreticulata* Stancheva. 14. LV, external view, ♂; 15. RV, external view, ♂; 16. LV, external view, ♀; 17. RV, external view, ♀; 18, 19. *Darwinula stevensoni* (Brady & Robertson); 18. LV, external view; 19. RV, external view.

b: The most representative ostracods from Seddülbahir and İntepe sections (late Miocene; late Bessarabian–Khersonian). 1–4. *Cyprideis torosa* (Jones); 1. LV, external view, ♀; 2. RV, external view, ♀; 3. LV, external view, ♂; 4. RV, external view, ♂. 5,6. *Cyprideis torosa* (Jones), specimens with tubercula; 5. LV, external view, ♀; 6. RV, external view, ♀; 7–11. *Euxinocythere (E.) immutata immutata* Stancheva; 7, 9. LV, external view; 8, 10. RV, external view; 11. C, dorsal view; 12–14. *Euxinocythere (E.) immutata bononiensis* Stancheva; 12. LV, external view; 13. RV, external view; 14. C, dorsal view; 15–17. *Euxinocythere (E.) topolensis* Stancheva; 15. LV, external view; 16. RV, external view; 17. C, dorsal view. 18, 19. *Xestoleberis fuscata* Schneider; 18. LV, external view; 19. RV, external view. 20, 21. *Xestoleberis castis* Mandelstam; 20. LV, external view; 21. RV, external view. 22, 23. *Loxoconcha rimopora* Suzin; 22. LV, external view; 23. RV, external view; 24. *Loxoconcha subcrassula* Suzin, LV, external view. 25. *Loxoconcha turgida* Stancheva, RV, external view. 26–29. *Loxoconcha* sp.; 26. LV, external view; 27. RV, external view; 28. C, dorsal view.

grey very fine-grained sandstone layer contains cm-scale cross-stratifications and abundant shell fragments, almost entirely of the bivalve *Chersonimactra bulgarica*. This unit is oxidised at the top where it displays a reddish colour. This transitional interval represents a flooding surface formed during a transgressive event separating 2 distinctive depositional environments (Fig. 6a).

The upper part of the section (4.5–41.5 m) displays an alternation between bluish-grey claystones to siltstones and yellowish medium-grained to very coarse-grained sandstones. This interval may be divided into 3 successions (Fig. 6a). These successions present at the base bluish-grey claystones to siltstones that commonly contain mm-thick horizontal laminations, shell fragments and dm- to m-scale layers of light grey very fine-grained calcareous sandstones with abundant shell fragments. Upwards, they often display cm-scale lenticular bedding or even cm-scale symmetric wavy bedding. These fine grained sediments highlight deposition out of suspension alternating with distal bottom-currents formed under storm and wave activity. They are interpreted to have been deposited in nearshore and shoreface environments. Further up section, coarser material becomes more abundant and the main lithology is formed by yellowish medium-grained to very coarse-grained sandstones and conglomerates. Sandstones typically contain mm-thick horizontal laminations, cm-scale symmetric wavy beddings, cm-scale trough-cross stratifications, cm-scale vertical burrows and/or cm-scale layers made of reddish silt-clay that commonly contain cm-scale terrestrial organic material fragments, cm-scale bone fragments and shells and shell fragments. The coarser grained sediments were deposited under lower stage plane-bed flow regime or by dune migration during channel infill in wave-worked foreshore or backshore environments. Sandstones are commonly covered by greenish-grey silty-clay with mm-thick horizontal laminations, cm-scale vertical burrows, cm-scale terrestrial organic material fragments, shell fragments and cm-scale bone fragments. These organic-rich sediments are often bioturbated and mottled. They highlight deposition from suspension in very low energy standing waters or sedimentation in lagoonal environments. The three successions represent regressions from nearshore, shoreface, foreshore, backshore, up to lagoon environments and may therefore be interpreted as regressive parasequences. The parasequences are separated by oxidised shell-rich lags composed of light grey very fine-grained sandstones containing abundant shell fragments and shells. These lags represent flooding surfaces formed during minor transgressive events. Overall, the upper part of the section shows a regressive trend, finally merging into a shoal-water delta, according to the Postma classification (Postma, 1990). Sediments are relatively fine-grained and mostly deposited in horizontal layers, typically recording planar laminations. They highlight deposition in relatively quiet, organic-rich, shallow water environments with a low-gradient slope, recording minor wave action and lacking tidal activity. Direct river influence on the deposition of the Seddülbahir section appears to have been restricted. These sedimentary characteristics are very similar to the Pliocene deltaic deposits of the Dacian basin of Romania (Jorissen et al., 2018).

The detailed sedimentary log of the 8-m long İntepe-2 section is

shown in Figs. 5, 6b. The lower part of the section (0–2.5 m) displays greenish-grey claystones to siltstones with mm-thick planar laminations of silt. Sediments are enriched in mm-scale terrestrial organic material fragments, cm-scale vertical roots and shell fragments, culminating (at 2 m) in a distinct 10 cm thick lignite bed (Fig. 5c). These sediments suggest deposition from suspension in very low energy standing water, interpreted as a lagoonal environment. These fine grained sediments are overlain by a coarse grained interval (2.5–3.5 m), which consists of a shell-rich lag composed of yellowish fine-grained sandstones. Sandstones contain mm-thick horizontal laminations and abundant shell fragments. This interval is interpreted as a flooding surface formed during a transgressive event. The base of the upper part of the section (3.5–8 m) is formed by yellowish very fine to fine-grained sandstones, containing cm-scale asymmetric wavy beddings and some shell fragments. Sediments suggest deposition under distal bottom-currents formed during storm and wave activity. Upwards, the section continues with brownish-grey claystones to fine sandstones, containing mm-thick planar laminations of silt and some shell fragments. Sediments highlight deposition out of suspension alternating with distal bottom-currents formed under storm and wave activity. Overall, the upper part of the section records a general regression, and sediments are interpreted to be deposited in nearshore environments.

## 5. Ostracods

### 5.1. Results

Most samples from the Seddülbahir section yielded a rich ostracod fauna that can be grouped into two assemblages (Fig. 7): The lower few meters of the section (0–4.5 m) are mainly composed of grey-greenish clays that contain an ostracod assemblage dominated by freshwater to oligohaline species like *Heterocypris formalis*, *Stanchevia* sp. and *Candona angulata* (Figs. 7, 8a,b). Ostracods are very abundant and even visible with the naked eye on the bedding planes. These taxa are associated with numerous individuals of the euryhaline species *Cyprideis torosa* as well as with the freshwater form *Ilyocypris bradyi*. This ostracod assemblage frequently occurs in levels rich in fresh-water as well as anomalohaline (brackish) mollusk species.

The upper part of the section contains an oligo- to lower mesohaline ostracod fauna suggesting a slight increase in salinity. The main ostracod species are represented by leptocytherids, i.e. *Euxinocythere (Euxinocythere) immutata immutata*, *E. immutata bononiensis*, *E. topolensis*, as well as loxoconchids like *Loxoconcha rimopora*, *L. subcrassula*, *L. turgida* and *L. sp.* associated with *Xestoleberis fuscata*, *X. castis* and *Cyprideis sublittoralis*.

The İntepe-2 section yielded a brackish ostracod association (samples IT01, IT04, IT05), dominated by *Cyprideis torosa*, *Euxinocythere (Euxinocythere) immutata immutata* and rare *Loxoconcha rimopora* (Fig. 7). The interval straddling the lignite layer (samples IT02, IT03), as well as the upper part of section (sample IT 06), provided rare freshwater ostracods such as *Limnocythere levisreticulata*, *Candona*





Fig. 8. (continued)

*neglecta*, *Candona angulata*, *Darwinula stvensoni*, and *Ilyocypris bradyi*, together with frequent shells of *Cyprideis torosa*.

## 5.2. Stratigraphic implications

The ostracod fauna from the Seddülbahir section unequivocally represents late Miocene Paratethyan assemblages. Similar ostracod assemblages were previously described by Stancheva (1972, 1976, 1984,

1990) from the upper Miocene (upper Bessarabian-Khersonian) deposits of northeastern Bulgaria, at the western coast of the Euxinian Basin, and from northwestern Bulgaria (Dacian Basin), both basins being components of the Eastern Paratethys at that time. Stancheva (1976, 1984) divided the Sarmatian s.l. stage of Bulgaria into six ostracod range zones: 1. *Cytheridea hungarica* - *Aurila mehesi* Zone (early Volhynian); 2. *Euxinocythere* (*E.*) *turpe* Zone (late Volhynian); 3. *Euxinocythere* (*E.*) *grave odessoensis* Zone (early-middle Bessarabian); 4.

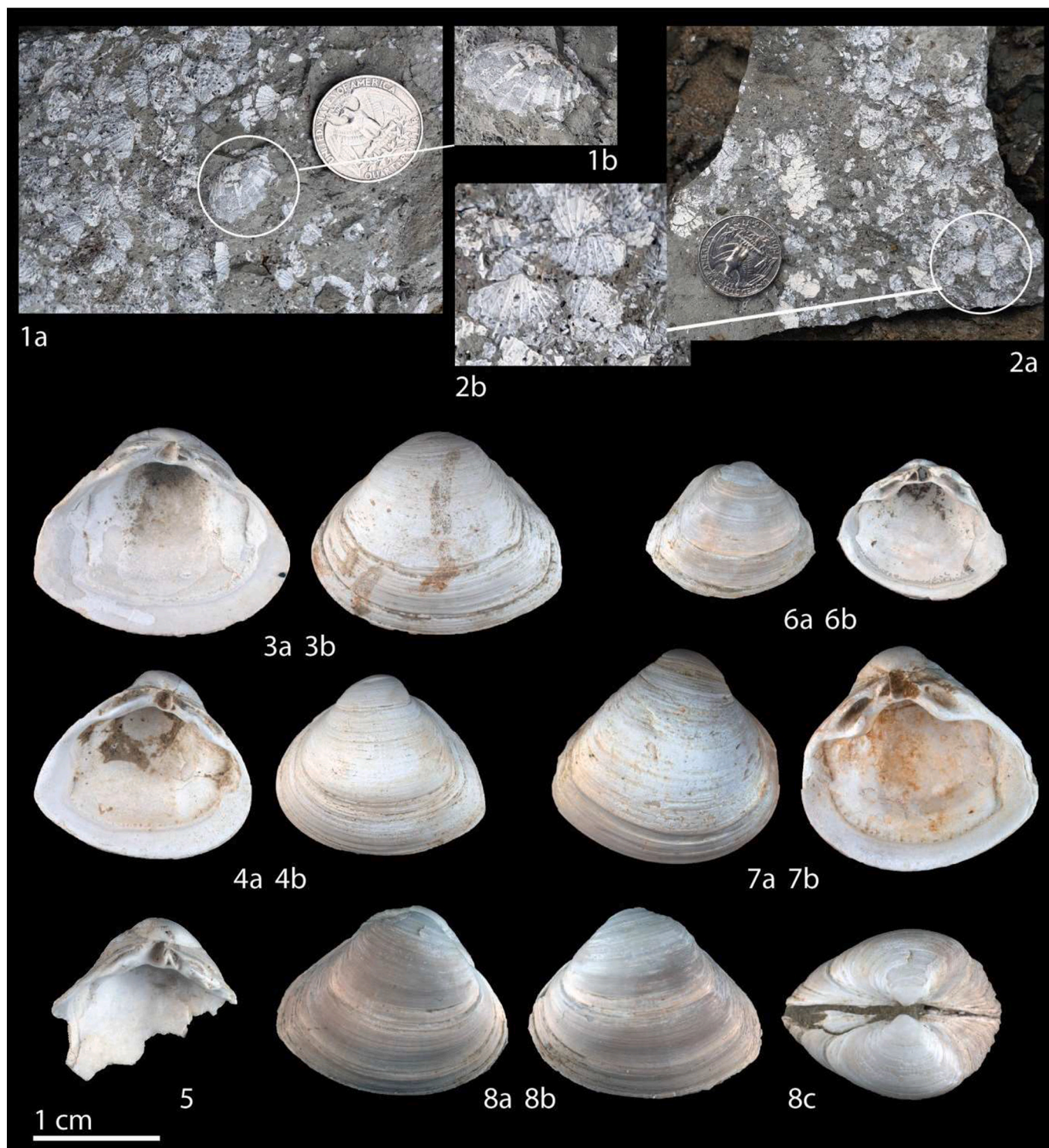


Fig. 9. Bivalvia. (1–2) *Plicatiformes* cf. *plicatiformis* (Sinzov, 1896), from basal strata of Seddülbahir section. (3–8) *Chersonimactra bulgarica* (Toula, 1892), from the interval 25–30 m, Seddülbahir. Note the presence of paired specimens, signifying in-situ preservation. Scale bar = 1 cm; the coin has a diameter of 24.26 mm.



*Loxoconcha subcrassula* Zone (late Bessarabian); 5. *Euxinocythere* (*E.*) *immutata* Zone (early Khersonian); 6. *Euxinocythere* (*E.*) *dilecta* Zone (late Khersonian).

The high frequency of leptocytherid species *Euxinocythere immutata* (with two subspecies) in the Seddülbahir section of the Alçıtepe Formation suggests an early Khersonian age (= *Euxinocythere* (*E.*) *immutata* Zone). The presence of *Loxoconcha subcrassula* and *L. rimopora* point towards a late Bessarabian age (= *Loxoconcha subcrassula* Zone) for the lower part of the succession. However, this part of the section contains fresh water ostracods, which are not very useful for precise dating, but do provide valuable palaeoenvironmental information.

Ostracods of the Neogene Gelibolu Basin have previously been studied by Tunoğlu and Ünal (2001a, 2001b) and Ilgar et al. (2012). They described an upper Miocene (early-middle Pannonian) ostracod assemblage from the lower part of the Çanakale Formation (Gazhanedere and Anafarta Members). The Pannonian regional stage is commonly used in the Central Paratethys, and is time equivalent with the middle Bessarabian-Khersonian and Maeotian-Pontian stages from the Eastern Paratethys (see Hilgen et al., 2012). Despite some taxonomic confusion - especially regarding the index species *Euxinocythere immutata* that was named *Paralimnocythere* sp. 1 and *P.* sp. 2 (Tunoğlu and Ünal, 2001b; Figs. 7–8) -, these ostracod assemblages have clear similarity with the species found in our studied section. The ostracods and floral associations in the Dardanelles sections represent environmental conditions similar to the Eastern Paratethys bioprovince and no Mediterranean affinities were detected.

Non-marine brackish (mesohaline) ostracods from the Lake

Küçükçekmece region, west of Istanbul, were analyzed by Witt (2010). He identified an ostracod assemblage from sediments of the late Miocene Ergene Formation, composed of leptocytherids (*Euxinocythere immutata*, *E. topolensis*) and loxoconchids (*Loxoconcha* sp. A, similar to *L. rimopora*) attributable to the late Miocene (Khersonian to Maeotian). This fauna shows clear affinities with the ostracod assemblage that we identified in the Seddülbahir section. Similar fresh to oligohaline ostracod species (despite of few taxonomic discrepancies) are mentioned by Şafak (2016) and Şafak and Güldürek (2017) from late Miocene sediments of the Ergene Formation from boreholes in the Edirne-Kırklareli area (Thrace region) and of the Bakırköy Formation south of Istanbul.

## 6. Mollusks

### 6.1. Results

The Seddülbahir section is dominated by oligohaline mollusk assemblages with only three bivalve species along with a terrestrial gastropod. Remnants of a very poorly preserved, extremely thin-shelled and unidentifiable unionoid were encountered in the basal organic-rich strata (0–3 m). The same interval also returned dense accumulations of poorly preserved Lymnocyprinae, which probably correspond to *Plicatiformes* cf. *plicatiformis* (Fig. 9; 1–2).

The most common mollusk species in Seddülbahir is the mactrid *Chersonimactra bulgarica*, originally recorded from the Khersonian of Balchik, Bulgaria. It occurs throughout almost the entire section, either

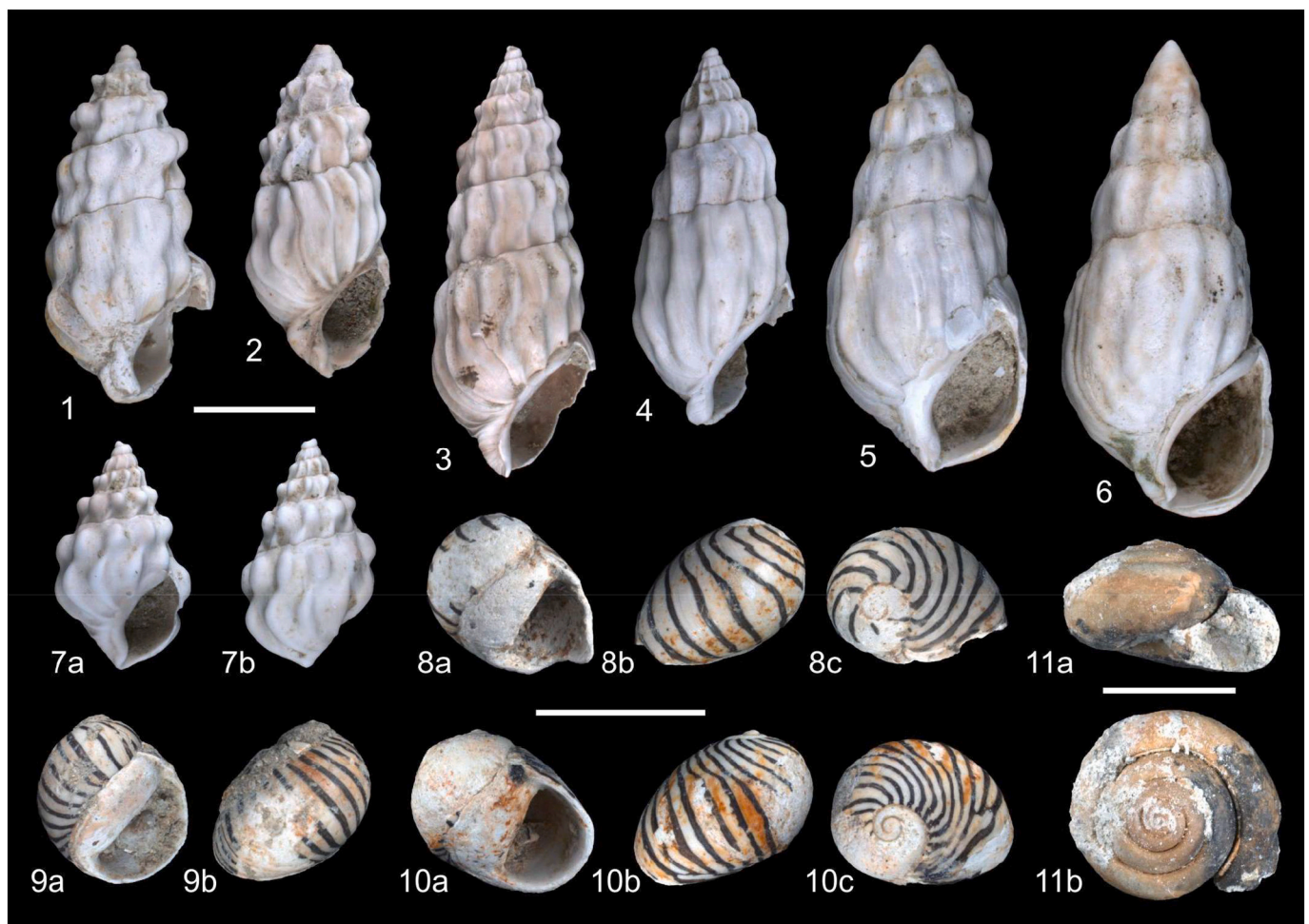


Fig. 10. Gastropoda. (1–7) *Melanopsis trojana* Hoernes, 1876, all from İntepe (northern section, above lignite); (8–10) *Theodoxus stefanescui* (Fontannes, 1887), from same section and position; (11) Internal cast of a stylommatophoran land snail, from Seddülbahir section. Scale bars = 5 mm.

as well preserved, individual shells (Fig. 9; 3–8) or in the form of dense, monospecific pavements in sandstone with the original shell material usually lacking. A land snail species (Fig. 10; 11) was retrieved from grey silts at the level of ~SB5. It belongs to the order Stylommatophora and resembles recent species of Oxylchilidae and Gastrodontidae (see Welter-Schultes, 2012), but the poor preservation as internal casts makes identification even at the family level impossible.

At İntepe-2, bivalves were only detected in the interval below the lignite horizon and include an unidentifiable unionoid and a species of Mactridae. The preservation of the mactrid is insufficient to identify in more detail, but the overall shape closely resembles the Seddülbahir material of *C. bulgarica*. The İntepe-2 section contains numerous specimens of the gastropod *Melanopsis trojana* (Fig. 10; 1–7). Additionally, a few specimens of *Theodoxus stefanescui* (Fig. 10; 8–10) were retrieved from the upper part of the section, above the lignite horizon.

Finally, a faunule consisting of *Melanopsis* cf. *trojana* and lymnocardiinae bivalves (?*Plicatiformes* cf. *plicatofittoni*) was encountered at the road section of Poyraztepe (40°12'20"N; 26°21'56"E). Specimens are embedded in a sandstone matrix, along with imprints of a pine cone and wood fragments, suggesting proximity to land.

## 6.2. Stratigraphic and taxonomic implications

*Plicatiformes plicatofittoni* was originally described from Bessarabian deposits of the Kherson district, Ukraine, and is characterised by distinct ribs that are usually ornamented by scales (Sinzov, 1896; Nevesskaya et al., 1993). The lack of such fine sculptural details in the Turkish material is likely the result of the poor preservation. A similar species is *Plicatiformes fittoni* from the Bessarabian of the Rostov region, Russia, which differs in the presence of distinct spikes on the rib-tops (see also Nevesskaya et al., 1993; Paramonova, 1994; Frolov et al., 2020). Earlier identifications as *Paradacna abichi* can be excluded based on the strongly inequilateral shell of that species (Hoernes, 1874; Nevesskaya et al., 1997).

*Melanopsis trojana* is only known from the area of İntepe. Hoernes (1876) originally described it from the locality “Renköi”, which is presently known as Erenköy and is part of İntepe. As for many other melanopsids, shell shape and sculpture is highly variable in *M. trojana*. The species can easily be confused with the Plio-Pleistocene *M. orientalis* from Greece or the Pliocene Croatian species *M. lanceolata*, which share the elongate shape and the distinct axial ribs that occasionally form tubercles close to the upper suture. *Melanopsis trojana* differs from those species in the comparably weak callus and the presence of a distinct fasciole.

*Theodoxus stefanescui* was described from the Maeotian of the Dacian Basin and shares with the Turkish specimens the subglobular shape, the thick callus pad and the colour pattern consisting of dark, wavy axial stripes (Wenz, 1942). A very similar species is *Theodoxus bessarabicus* from the Bessarabian of Moldova, which shares the low apex and the thickened callus pad, but differs in the presence of denticles on the callus pad and a zigzag pattern. Given the overall morphological similarity both species might belong to the same lineage. *Theodoxus scamandri*, which is the only *Theodoxus* species described from the Miocene of the Çanakkale region, has a similarly thick callus pad and low apex but differs in the distinctly wider shell with broader aperture, the weakly denticulate callus and the dense zigzag pattern.

## 7. Calcareous nannofossils and ascidian spicules

### 7.1. Results

The calcareous nannofossil assemblages in the 19 smear-slides all show moderate or poor preservation, and specimens occur in variable abundance; two samples (IT2, IT3) are barren. Semi-quantitative abundance evaluation of the observed nannofossil specimens is reported in Table 1. In most of the samples, assemblages are made up of

reworked forms, dominated by few to common specimens of placoliths belonging to genera *Clausicoccus*, *Coccolithus* (*C. eopelagicus*, *C. miope-lagicus*, *C. pelagicus*), *Cribrocentrum*, *Cyclicargolithus*, and *Dictyococcites*, largely represented by long-range taxa among which it is not possible to discriminate in situ components. Scattered and rare specimens of typical Palaeogene nannofossils are also present (e.g., *Discoaster barba-diensis* in fragments, *Ericsonia formosa*, *Helicosphaera recta*, *H. lophota* group, *Reticulofenestra dictyoda*, *R. umbilicus*, *Sphenolithus ciperoensis* and *S. radians*), and very rare lower to middle Miocene *Helicosphaera* species (*H. walbersdorfensis* and *H. orientalis*) in few samples (e.g. SB9). In the İntepe-2 section, few reworked calcareous elements belonging to the so-called ascidian spicules (*Micrascidites*, *Perfocalcinella* and *Lac-nolithus*) have been observed in samples IT3 and IT4. These calcareous ascidian spicules are generally present in shallow marine environments and can occur within nannofossil assemblages, as observed in Black Sea sediments (Golovina et al., 2019).

### 7.2. Stratigraphic implications

In both Seddülbahir and İntepe-2 sections, age-diagnostic taxa have not been observed, and assemblages are dominated by a mixing of reworked taxa from the late Eocene and Oligocene, with a very low percentage of early Miocene reworked forms. The claimed presence of Messinian-Zanclean age-diagnostic taxa in the Alçitepe formation by Melinte-Dobrinescu et al. (2009) is not replicated. It is to be noted that their taxonomic assignments of single or very rare specimens to the biostratigraphic marker species *Ceratolithus acutus*, *Triquetrorhabdulus rugosus*, *Reticulofenestra rotaria*, *Nicklithus amplificus*, and *Amaurolithus primus* (documented on Plate 1 in Melinte-Dobrinescu et al., 2009) is highly questionable. Poor preservation of nannofossils and the irregular morphology of the type specimens of some of the quoted taxa (e.g. *C. acutus*, *N. amplificus*, *T. rugosus*) do not justify this attribution. Moreover, in these shallow water sediments it would be surprising to find markers that are usually rare in rich assemblages from fully marine open-ocean sediments, such as *C. acutus* or *T. rugosus*, but not to find any of the other components of the upper Miocene-lowermost Pliocene assemblage, represented by long-range taxa. Similar considerations were made regarding the analyses of nannofossil remnants in Black Sea cores and sections (Van Baak et al., 2015; Golovina et al., 2019), in which the supposed specimens of *C. acutus* found by Popescu (2006) were not observed and most probably represent fragments of ascidian spicules (see discussion in Golovina et al., 2019).

**Table 1**  
Nannofossil data

Seddülbahir section			İntepe section		
Sample	Total nannos N/ mm <sup>2</sup>	Other fossils	Sample	Total nannos N/ mm <sup>2</sup>	Other fossils
SB11	315	–	IT6	162	–
SB10	204	–	IT5	47	–
SB9	334	–	IT4	32	Ascidians
SB8	207	–	IT3	0	–
SB7	242	–	IT2	0	Ascidians
SB6	366	–	IT1	76	–
SB5	313	–			
SB4bis	102	–			
SB4	33	–			
SB3	11	–			
SB2	32	–			
SB1	33	–			



## 8. Aquatic and terrestrial palynology

### 8.1. Results

The aquatic signal in sample SB2 is dominated by *Pediastrum* (freshwater colonial algae) with occasional *Botryococcus* (mainly fresh water but can be tolerant of oligohaline-lower mesohaline conditions; Mudie et al. (2010)). No dinocysts were observed (in situ or reworked). The terrestrial signal consists primarily of *Pinus*, along with occasional occurrences of other conifers (e.g. *Cedrus*, *Tsuga* and *Abies*), deciduous trees (e.g., *Carya*, *Alnus*, *Carpinus*, *Fagus*) and rare pollen of herbaceous plants (e.g., Lactuicoideae and Caryophyllaceae). The pollen signal is dominantly arboreal.

Sample SB4 shows dominantly terrestrial influence, including pollen of *Pinus*, *Cedrus*, *Quercus*, *Carya*, *Ulmus-Zelkova*, *Carpinus*, Asteroideae, Lacticoideae and Amaranthaceae. Abundant plant material is also present, including leaf fragments. The aquatic signal is represented by occasional *Botryococcus* and rare spiniferate cysts, possibly *Spiniferites*, but with extremely reduced trifurcate processes. A single corroded specimen was observed of a wetzeliellid dinocyst (but with uncertain attribution due to corrosion of diagnostic features), probably reworked from Palaeogene deposits. Additionally, a discoloured chorate cyst was observed but could not be identified due to heavy corrosion.

Sample SB4B shows good preservation of terrestrial material such as leaf and woody fragments, indicating relatively large amount of terrestrial input. Pollen is present including *Pinus*, *Cedrus*, *Picea*, *Carpinus* and Asteraceae, but some grains (including one taxodiaceous Cupressaceae grain and one Asteroideae grain) show extremely dark (bronzed) exines relative to the more transparent looking in situ pollen, indicating that they have been heated and/or reworked (see Hoyle et al., 2018). Other reworking includes a single specimen of the dinocyst genus *Deflandrea*, which has an early Miocene (Aquitian) Last Appearance Datum (Hilgen et al., 2012) and is therefore probably reworked. A *Classopollis* tetrad was observed (reworked from the Mesozoic). The only aquatic palynomorphs that are not definitely reworked are occasional *Botryococcus* and a single small unidentified spiny acritarch.

Sample SB11 has very poor retrieval with only rare pollen grains of *Pinus*, Asteroideae and Lactuicoideae, and a single corroded grain of

*Ulmus-Zelkova*. Although some of the *Pinus* grains show transparent exines and clear detail of the corpora and sacchi, others have extremely dark and corroded exines, heavily suggestive of origins in older rock strata via one or multiple phases of heating and/or sedimentary reworking. Occasional remains of terrestrial plants such as leaf cuticle fragments occur as well. A single specimen was seen of a spiniferate dinocyst with extremely reduced trifurcate processes. An extremely discoloured/corroded fragment of a chorate dinocyst was also observed, suggestive that it has been reworked from older sediments. A single dinocyst operculum, consisting of a hexagonal plate with < 6 small bifurcate processes, was also observed but could not be identified with certainty as the main part of the cyst was absent.

### 8.2. Environmental implications

The aquatic environment of the lowermost part (0–4.5 m; SB2) of the Seddülbahir section unambiguously indicates a freshwater depositional setting, with dominance of *Pediastrum* and *Botryococcus*. Pollen assemblages represent various vegetation types in the terrestrial realm, including mid-altitude conifer forests and deciduous forests, with subsidiary representation of herbs, which may have formed the understory to the dominant forests, or may represent steppe assemblages from further afield. The aquatic environment characterising the upper part of the Seddülbahir section in SB4 cannot be reliably reconstructed due to the scarcity of dinocysts and other aquatic palynomorphs, but the presence of *Botryococcus* and the extremely reduced processes on the spiniferate cysts (if they are in situ) suggests at least some fresh water influence.

Palynological indicators of the palaeoenvironment in the İntepe samples are sparse, but the presence of *Pediastrum* suggests freshwater deposition. Palaeoenvironment cannot be specified in detail, as no definitive aquatic palynomorphs were observed, but terrestrial influence was significant.

## 9. Mammals

### 9.1. Results

The fossiliferous level at Seddülbahir yielded a small assemblage of

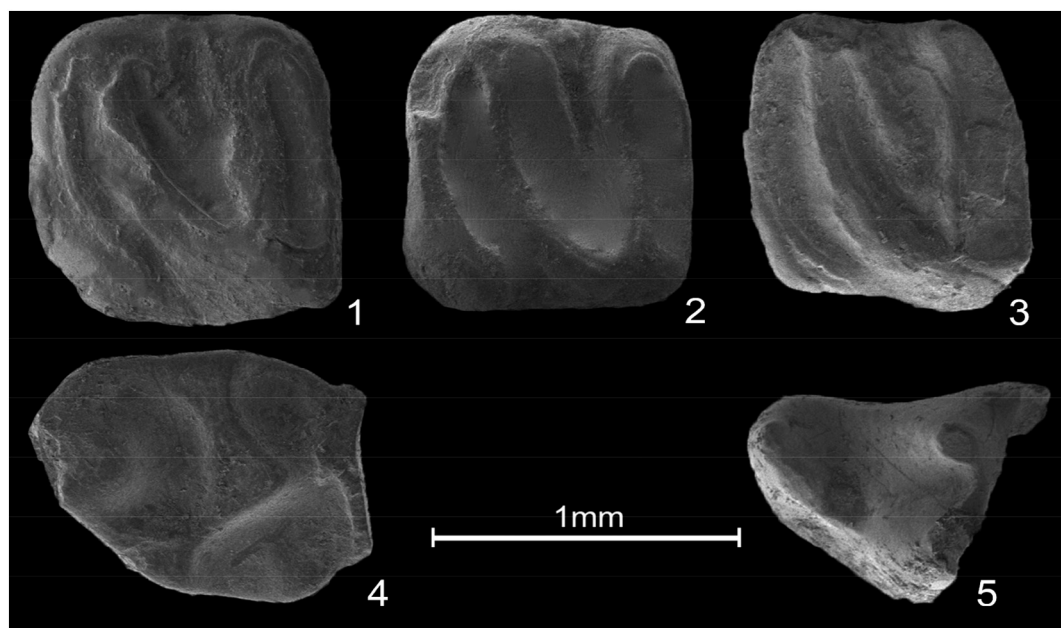


Fig. 11. Mammals from Seddülbahir. (1–3) *Myomimus dehmi/maritsensis* M1 dext. (PV 14980–982); (4) Murinae gen. et sp. indet M1 dext. (PV 14983); (5) *Eulipotyphla* indet. Trigonid m1 sin. (PV 14984). Note that damage to the enamel suggests the assemblage has been reworked.

mammal remains that shows evidence of having been reworked (Fig. 11). Five molars were recovered. A heavily worn m1 of a murid could be identified to the family level only. An insectivore trigonid could not be identified, but is most reminiscent of a talpid. The other three molars, all M1/M2 ( $0.94 \times 1.07$ ,  $0.96 \times 1.08$ ,  $0.95 \times 1.06$ ) belong to the glirid *Myomimus* and more specifically to the *M. dehmi*-*M. maritsensis* lineage, two species that can mainly be distinguished on the morphology of the P4/p4 (Daxner-Höck, 1995). Morphologically, the more simplified molars fit better with *M. maritsensis*. However, they are somewhat smaller than the material assigned to that species from Maramena (MN 13; Daxner-Höck, 1995) and are even below the range of the width of that locality. The same goes for the Turolian locality of Hayranlı (MN 11/12), also assigned to *M. maritsensis* (Kaya and Kaymakçı, 2013). The sizes fit better with material from MN12 Moldavian localities assigned to *M. dehmi*/*maritsensis* by Delinschi (2013) or the *M. dehmi* assemblages from Tuğlu (MN 9; Joniak and de Bruijn, 2015).

Evidence of reworking is most obvious in the murid M1. The anterocone complex is sheared off and the resulting surface is polished. Polishing is also seen in a rodent incisor, in which only patches of enamel have been preserved on the oral surface. Possibly because of their sturdy build, the *Myomimus* molars seem to be less affected, but, here too, the enamel of the ridges is partly polished off. Insectivore molars are notoriously fragile and the presence of a fresh looking trigonid fragment in the assemblage is somewhat surprising. Possibly this is an admixture to the reworked material from the fauna living at the time of deposition.

Having an assemblage that has been reworked only poses a lower limit to the age of the layer. Given the scantiness of the material, even that age carries uncertainty. The only indication we have is the stage of evolution of the *Myomimus* molars, which morphologically fit *M. maritsensis* but are metrically a better match with *M. dehmi*. The transition from *M. dehmi* to *M. maritsensis* can not be exactly pinpointed, but took place in the earlier part of the Turolian.

## 9.2. Stratigraphic implications

A late Miocene age for the small mammals of Seddülbahir fits well with the ages of various other mammal faunas from the Kirazlı and Alçitepe formations (Table 2). An extensive literature review shows that eight fossil mammal localities have previously been described from the Kirazlı and Alçitepe formations (Fig. 2; Table 2; Supplementary material). The oldest faunas, from the basal part of the Kirazlı Formation, correlate to MN 8 providing ages between 13.3 and 11.2 Ma (Kaya, 1982, 1989; Ünay et al., 2003; Koufos et al., 2018; Pickford et al., 2020). The localities from the upper part extend up to MN 10 indicating an age range between 9.9 and 8.9 Ma (Calvert and Neumayr, 1880; Kaya, 1989; Saraç, 2003; Şen, 2016; Koufos et al., 2018). Mammal localities of the Alçitepe Formation are all attributed to the lower-middle Turolian with ages between 8.9 and 6.8 Ma (Ünay and De Bruijn, 1984; Kaya, 1989). All this indicates that the Kirazlı-Alçitepe transition should roughly be located within the MN10–11 zones, which comprise an age range of 9.9–7.6 Ma.

**Table 2**  
Fossil mammal data

Code	Site	Formation	Biozone	Age (in Ma)	Reference
1	Nebisuyu	Kirazlı	MN 8	13.3–11.2	Kaya (1982, 1989); Pickford et al. (2020)
2	Kabatepe	Kirazlı	MN 8	13.3–11.2	Saraç (2003)
3	Bayraktepe-1	Kirazlı	MN 8	13.3–11.2	Koufos et al. (2018); Ünay et al. (2003)
	Bayraktepe-2	Kirazlı	MN 9	11.2–9.9	Koufos et al. (2018); Ünay et al. (2003)
4	Sığındere	Kirazlı	MN 10	9.9–8.9	Kaya (1989); Koufos et al. (2018); Saraç (2003)
5	Erenköy	Kirazlı	MN 8–11	13.3–7.6	Calvert and Neumayr (1880); Şen (2016)
6	Değirmendere	Alçitepe	MN 11–12	8.9–6.8	Kaya (1989)
7	Bayırköy	Alçitepe	MN 12	7.6–6.8	Ünay and De Bruijn (1984)

## 10. Strontium isotope geochemistry

All the Sr isotope ratios from the Seddülbahir and İntepe sections (Table 3) are substantially lower than contemporaneous open-marine values (Fig. 12). The new ratios cluster in two groups (values about 0.7083 and about 0.7087). The group with the lowest  $^{87}\text{Sr}/^{86}\text{Sr}$  values of  $\sim 0.7083$  comprise the samples IT1 and SB10 and samples from the Zelenka section of the Bulgarian margin. These values are similar to the  $^{87}\text{Sr}/^{86}\text{Sr}$  data of Maeotian samples of the Black Sea (Zheleznyi Rog section) and Caspian Sea (Adzhiveli section) basin (Grothe et al., 2020), and may be characteristic for an isolated Eastern Paratethys water mass in late Miocene times. The second group, comprising samples IT3, IT6 and SB1, have significantly higher  $^{87}\text{Sr}/^{86}\text{Sr}$  values of  $\sim 0.7087$ . Variation between these samples is relatively small, indicating a stable  $^{87}\text{Sr}/^{86}\text{Sr}$  ratio throughout this period.

## 11. Discussion

### 11.1. Age of the Kirazlı-Alçitepe formations

The ostracod and mollusk assemblages found at Seddülbahir and İntepe-2 represent a typical late Bessarabian-Khersonian succession showing that instead of a Messinian-Zanclean transition as proposed by Armijo et al. (1999) and Melinte-Dobrinescu et al. (2009) these sections are actually about 4 million years older. The presence of *Loxococoncha subcrassula* and *L. rimopora* at the basal part (0–4.5 m) of the Seddülbahir section indicates a latest Bessarabian or early Khersonian age. The abundance of leptocytherid species *Euxinocythere immutata* (with two subspecies) in the section also points to a Khersonian age. The bivalves from Seddülbahir show a similar biostratigraphic signal as the ostracods. *Plicatiformes* cf. *plicatofittoni* suggests a Bessarabian age for the basal part of the section, while *Chersonimactra bulgarica* denotes a Khersonian age. The melanopsids at İntepe are endemic to the region and thus of no biostratigraphic value. *Theodoxus stefanescui* is typical for the Maeotian of the Dacian Basin, but has also been mentioned from late Bessarabian and Khersonian strata of Romania and Turkey (Stefanescu, 1896; Rückert-Ülkümen et al., 2006). The Seddülbahir mammal assemblage is estimated to represent the earlier part of the Turolian, which corresponds with the results from the ostracod and mollusk assemblages.

The Bessarabian-Khersonian transition is estimated to have an age of 8.9–8.6 Ma (Palcu et al., 2019b). The Khersonian of the Black Sea comprises the oceanic diatoms *Thalassiosira burckliana* and *Nitzschia fossilis* (Radionova et al., 2012), that have global first occurrences of 8.9 Ma, according to Barron and Badlauf (1995). The Bessarabian-Khersonian boundary in the Dacian Basin is estimated older than 8.5 Ma, as the reversed polarity chron C4r.2r is found in Khersonian deposits (Vasiliev et al., 2004; Palcu et al., 2019b). The top of the Khersonian is dated at several localities at 7.6 Ma (e.g. Filippova and Trubikhin, 2009; Rybkina et al., 2015; Palcu et al., 2019b).

We consider it possible that the observed increase in salinity at level 4.5 m in the Seddülbahir section actually corresponds to the Bessarabian-Khersonian transition, an interval that is marked by



**Table 3**  
Strontium isotope data

Code	Section	Paratethys stages	Age	Age estimate	$^{87}\text{Sr}/^{86}\text{Sr}$	2 $\sigma$ error	Reference
SB1	Seddülbahir	Bessarabian-Khersonian	9–8	8,7	0,708,662,713	1,32E-05	This study
SB10	Seddülbahir	Bessarabian-Khersonian	9–8	8,6	0,708,233	8,63E-06	This study
IT1	İntepe	Bessarabian-Khersonian	9–8	8,85	0,708,282,118	5,52E-06	This study
IT3	İntepe	Bessarabian-Khersonian	9–8	8,83	0,708,710,498	6,38E-06	This study
IT6	İntepe	Bessarabian-Khersonian	9–8	8,81	0,708,719,402	3,12E-05	This study
ZK10	Zelenka	Bessarabian-Khersonian	9–8	8,6	0,708,300,715	8,34E-06	This study
ZK18	Zelenka	Bessarabian-Khersonian	9–8	8,5	0,708,314,117	1,16E-05	This study
I-16	Yenimahalle	Pontian	6.1–5.6	5.6	0,70,827	1,98E-05	Çağatay et al. (2006)
I-20	Yenimahalle	Pontian	6.1–5.6	5.7	0,708,379	2,13E-05	Çağatay et al. (2006)
I-26	Yenimahalle	Pontian	6.1–5.6	5.8	0,708,281	1,98E-05	Çağatay et al. (2006)
I-37	Yenimahalle	Pontian	6.1–5.6	5.9	0,708,729	1,84E-05	Çağatay et al. (2006)
I-37	Yenimahalle	Pontian	6.1–5.6	5.9	0,708,723	1,56E-05	Çağatay et al. (2006)
I-37	Yenimahalle	Pontian	6.1–5.6	5.9	0,708,656	2,13E-05	Çağatay et al. (2006)
I-37	Yenimahalle	Pontian	6.1–5.6	5.9	0,708,715	1,56E-05	Çağatay et al. (2006)
I-39	Yenimahalle	Pontian	6.1–5.6	6.0	0,708,836	1,70E-05	Çağatay et al. (2006)
TR23	Zheleznyi Rog	Maeotian	6.2–7.6	7.75	0,708,084	1,00E-05	Grothe et al. (2020)
TH36	Zheleznyi Rog	Maeotian	6.2–7.6	7.2	0,708,234	9,00E-06	Grothe et al. (2020)
TR27	Zheleznyi Rog	Maeotian	6.2–7.6	6.7	0,708,228	1,00E-05	Grothe et al. (2020)
TR30	Zheleznyi Rog	Maeotian	6.2–7.6	6.55	0,708,286	8,00E-06	Grothe et al. (2020)
TR71	Zheleznyi Rog	Maeotian	6.16	6.16	0,708,284	1,60E-05	Grothe et al. (2020)

increased aridity in the Paratethys region (Palcu et al., 2019b). Consequently, our best age estimate for the Kirazlı-Alçıtepe boundary is about ~9 Ma. These ages are in good agreement with the absolute age control of a volcanic deposit (Taştepe basalt) in the Kirazlı Formation which provided radio-isotopic ages of  $10.1 \pm 0.2$  and  $9.5 \pm 0.3$  Ma (Ercan et al., 1995).

Our biostratigraphic data are clearly at odds with the Pliocene (younger than 5.3 Ma) age for the same sections by Melinte-Dobrinescu et al. (2009). They base their young age entirely on Mediterranean nanofossil assemblages. More specifically, they reported the presence of several marker species that are inconsistent with our Khersonian age for the Alçıtepe Formation: *Amaurolithus primus* (First Appearance Datum (FAD): 7.424 Ma), *Reticulofenestra rotaria* (FAD: ca. 7.41 Ma), *Nickolithus* (= *Amaurolithus*) *amplificus* (FAD: 6.909 Ma), and *Ceratolithus acutus* (FAD: 5.345 Ma). In their İntepe section, straddling the lignite bed, they reported *Amaurolithus primus*, *Reticulofenestra rotaria*, and *Ceratolithus acutus*. In the Seddülbahir section, however, only the presence of *C. acutus* is in stratigraphic conflict with our results. We re-examined exactly the same interval in the Seddülbahir section, but our nanofossil analyses did not confirm the presence of this enigmatic marker species. We also re-sampled the stratigraphic interval of the lignite bed in our İntepe-2 section. Also there we could not confirm the

presence of the three late Messinian-early Zanclean marine nanofossil markers. This is consistent with an overall dominance of fresh water indicators in the section. In conclusion, we cannot reproduce the biostratigraphic results of Melinte-Dobrinescu et al. (2009) and the assembled new evidence clearly shows that the two sections represent a time interval between ~10 and 7.6 Ma.

## 11.2. Palaeoenvironment and palaeoecology

All data from the lowermost part of the Seddülbahir section indicate the dominance of freshwater to oligohaline environments. The ostracod assemblage is dominated by freshwater to oligohaline species like *Heterocypris formalis*, *Stanchevia* sp. and *Candona angulata*, together with individuals of the euryhaline species *Cyprideis torosa* and the freshwater species *Ilyocypris bradyi*. The unionid mollusk remains also clearly indicate a strong freshwater influence. Extant unionoid species are typically restricted to moving and standing freshwater bodies. Many species are intolerant to elevated salinities, with 6 ppt being at the upper limit (Verbrugge et al., 2012; Johnson et al., 2018). The successors of lymnocyprinae bivalves found at this interval are presently limited to the Pontocaspian region, inhabiting oligohaline to mesohaline waters of the Caspian Sea and limans of the northern Black Sea

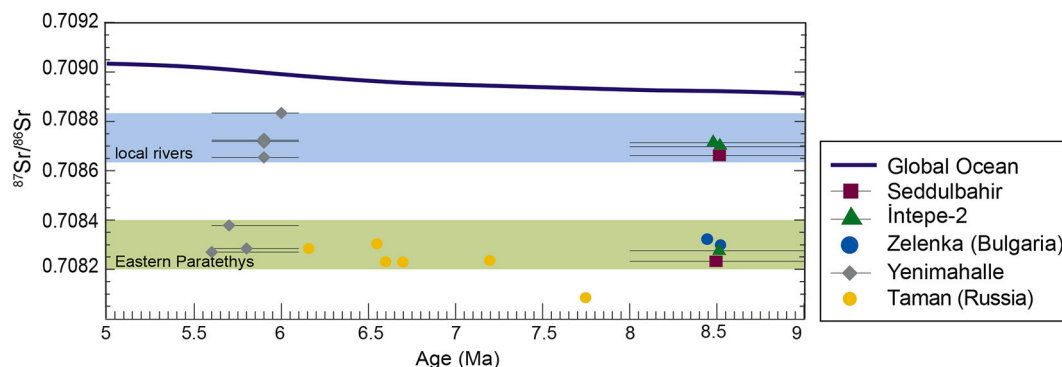


**Fig. 12.** Late Miocene  $^{87}\text{Sr}/^{86}\text{Sr}$  isotope data for the sections and sites in the Dardanelles and Paratethys region. Global Ocean water: McArthur et al., 2012; Seddülbahir, İntepe-2 and Zelenka are from this study; Yenimahalle section: Çağatay et al. (2006); Taman section (Russian Black Sea coast): Grothe et al. (2020). In light blue are the average values from fresh water environments interpreted to reflect local river water, in green are the values from anomalohaline environments interpreted as average values of an isolated Eastern Paratethys (Grothe et al., 2020). Note that the exact age of the individual samples from the Seddülbahir, İntepe-2, Yenimahalle and Zelenka sections is not known. We tentatively place the samples of Seddülbahir and İntepe-2, at around 8.5 Ma given their stratigraphic position. The black line indicates the age uncertainty (see Table 3 for details). (For interpretation of the references to colour in this figure legend, the reader is referred to the web version of this article.)

with one species (*Monodacna colorata*) extending well into lower courses of major rivers (Bogutskaya et al., 2013; Wesselingh et al., 2019). Additional arguments for a fresh aquatic signal in this interval are the dominance of the freshwater algae *Pediastrum* and the occasional presence of *Botryococcus* (mainly fresh water but can be tolerant of oligohaline-lower mesohaline (Mudie et al., 2010)). Fossil mammal remains at the uppermost level (4.5 m) of the lower part of Seddülbahir section indicate proximity to land. The  $^{87}\text{Sr}/^{86}\text{Sr}$  ratio for this lower interval (0.708663) is clearly below the marine curve and well above the general Paratethys ratios (Fig. 12). Given that the interval contains freshwater fauna, this  $^{87}\text{Sr}/^{86}\text{Sr}$  ratio suggests a dominance of local riverine waters as the main hydrological source for the Dardanelles basin.

The Seddülbahir section shows a conspicuous palaeoenvironmental change at level 4.5 m, which is sedimentologically represented by a flooding surface formed during a transgressive event. Our palaeoenvironmental reconstructions based on ostracod and mollusk assemblages suggest an increased salinity for the upper part of the section. This part contains a monospecific *Chersonimactra bulgarica* fauna and oligo- to lower mesohaline ostracod fauna represented by leptocytherids and loxoconchids (Fig. 7). *Chersonimactra* is an extinct Khersonian genus, endemic to Eastern Paratethys, a shallow water infaunal filter feeder, preferring sandy bottoms and probably tolerating mesohaline conditions between 4 and 10–12 ppt (Paramonova, 1994). The  $^{87}\text{Sr}/^{86}\text{Sr}$  ratio for this upper interval (0.708233) is much lower than the value for the lower section. This implies that increased salinity was not driven by additional marine Mediterranean influx, because inflow of such waters would increase  $^{87}\text{Sr}/^{86}\text{Sr}$  ratios. The strontium ratio of the upper part is, however, in good agreement with the  $^{87}\text{Sr}/^{86}\text{Sr}$  ratios of the Zelenka section of the Eastern Paratethys (Fig. 12) and the Maeotian ratios for a unified and isolated Paratethys Sea (Grothe et al.,

2020). We therefore infer that Paratethys was the main water source for the Khersonian Dardanelles basin.

At İtepe-2, the *Macra*-bearing level IT1, which also contains an ostracod fauna indicative of oligohaline water conditions, has similar characteristically low  $^{87}\text{Sr}/^{86}\text{Sr}$  value as Paratethys ratios. The faunal elements of the İtepe-2 section above the lignite layer suggest a dominance of fresh to oligohaline conditions. Melanopsid gastropods are found in variety of habitats in fresh to brackish water (Glaubrecht, 1996; Neubauer et al., 2016). *Theodoxus* is usually bound to freshwater as well, with few exceptions (Verbrugge et al., 2012; Glöer, 2019; Sands et al., 2019). Strontium isotopic ratios of IT3 and IT6 are similar to the freshwater part of the Seddülbahir section, supporting again the dominance of local riverine water sources.

### 11.3. Palaeogeographic and tectonic implications

Our biostratigraphic and palaeoenvironmental data of the Kirazlı-Alçıtepe formations shows that during Bessarabian-Khersonian times the Dardanelles region was intermittently changing from a local fresh-oligohaline lake to a mesohaline embayment of the Eastern Paratethys (Fig. 13). A similar change from fresh to more saline water was previously also documented in the *Chersonimactra*-bearing sediments of the Yenimahalle section that comprises the uppermost part of the Alçıtepe Formation at the Biga Peninsula (Çağatay et al., 2006). The  $^{87}\text{Sr}/^{86}\text{Sr}$  strontium ratios in the brackish upper part of Yenimahalle (I-16, I-20, I-26) are within the same Paratethys range, the ratios from the lower fresh water part (I-37, I-39) are much higher and agree very well with the  $^{87}\text{Sr}/^{86}\text{Sr}$  ratios of our freshwater sections (Fig. 12). Assuming that the hinterland source area did not change over this interval we estimate the  $^{87}\text{Sr}/^{86}\text{Sr}$  values of the local rivers draining into the Dardanelles basin at  $\sim 0.7087$ .

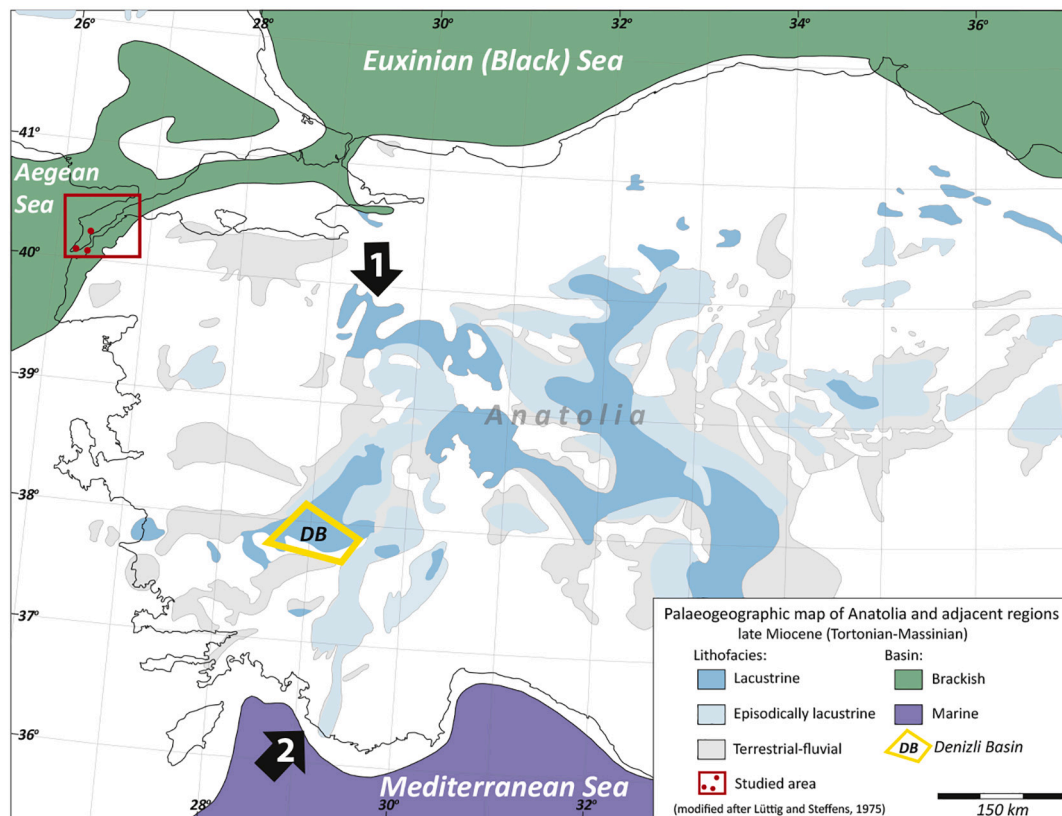


Fig. 13. Palaeogeographic map of western Turkey, modified by Lazarev et al. (2020) after Lüttig and Steffens (1976), showing the Dardanelles region as an embayment of the Eastern Paratethys in late Miocene times. The Denizli Basin in SW Turkey is the southernmost extent where Paratethyan fauna have been observed before the Lago Mare phase of the Messinian salinity crisis. How this fauna migrated to Denizli is still a major enigma (Rausch et al., 2020; Lazarev, 2020). Two hypothetical migration routes are explained by the arrows 1 and 2.



The  $^{87}\text{Sr}/^{86}\text{Sr}$  values of the intervals with anomalohaline Paratethyan fauna in the İntepe-2, Seddülbahir and Yenimahalle sections all indicate a dominant Paratethyan water source. This proves that the Dardanelles region must have formed, at least temporarily, an embayment of the Eastern Paratethys or that it was even part of a Bessarabian-Khersonian gateway connecting the Eastern Paratethys with the Northern Aegean (Popov et al., 2006; Krijgsman et al., 2020). The existence of such a gateway was previously documented in regional palaeogeographic maps (e.g., Lüttig and Steffens, 1976; Fig. 13) and may help to explain the enigmatic presence of late Miocene Paratethyan mollusk and ostracod species in the lacustrine deposits of the Denizli Basin of southwestern Turkey (Lazarev, 2020; Rausch et al., 2020).

Our new age constraint of 8.9–8.6 Ma for the Kirazlı-Alçıtepe transition also sheds another light on the evolution of the North Anatolian Fault (NAF), the major E-W trending strike-slip fault zone across Turkey (Fig. 1) that initiated as an escape structure following Arabia-Anatolia collision (Şengör et al., 2005). Originally it was suggested to propagate from eastern Turkey in the middle Miocene (~13 Ma) to the Marmara/Dardanelles region in the Pliocene (~5 Ma) (Armijo et al., 1999). According to Şengör et al. (2005, 2014), however, the NAF developed during the late-middle Miocene (12–11 Ma) in the Dardanelles region as a shear zone, whereas its localization as a transform plate boundary occurred during the Pliocene (Le Pichon et al., 2016). Recently, it was claimed that the current strike-slip regime of the entire NAF initiated already in the late Miocene, at an age of  $11.4 \pm 2.4$  Ma, and that east-west propagation may not have taken place (Nuriel et al., 2019). The Pliocene age of NAF initiation in the Dardanelles region is mainly based on the hypothesis that the Alçıtepe Formation post-dates the MES (Armijo et al., 1999; Karakaş et al., 2018). Here, we have shown that this formation is about 4 Myr older than previously reported, which implies that, if the tectonic reconstructions in the region are correct, the age the NAF initiation in the Dardanelles domain is approximately 9 Ma.

#### 11.4. The myth of the Messinian Dardanelles

All our palaeontological results indicate a late Miocene, Bessarabian-Khersonian age for the Kirazlı-Alçıtepe formations, suggesting deposition occurred between ~10 and 7.6 Ma. This is significantly older than in the conventional late Miocene chronostratigraphic framework of the Dardanelles basin (Fig. 3). Several stratigraphic schemes place the Kirazlı-Alçıtepe boundary in the lower Messinian (e.g. Görür et al., 1997; Çağatay et al., 2006), which in Eastern Paratethys terminology corresponds to the Maeotian. However, no Maeotian fauna has been described from these sedimentary successions, indicating that a thorough re-analysis of the entire Alçıtepe formation will be necessary to understand the Messinian evolution of the Dardanelles region. We also do not find any evidence for a Zanclean marine flooding as proposed by Melinte-Dobrinescu et al. (2009). All palaeontological indicators instead reveal fresh to brackish water environments, with evidence for terrestrial proximity. Our  $^{87}\text{Sr}/^{86}\text{Sr}$  values (0.7082) for the levels with highest salinity are far below the open ocean curve. They indicate that the Dardanelles region was probably connected to the Eastern Paratethys basin, at least during times when deposition took place in anomalohaline environments.

In addition, we could not confirm any major erosional unconformity in the Kirazlı-Alçıtepe formations. The lignite bed in the İntepe region, which was interpreted as key evidence for a Messinian unconformity by Melinte-Dobrinescu et al. (2009), is in our view a layer that fits very well in the dominantly fresh-water succession. The MES could not be confirmed at the Seddülbahir section either, and there is no difference in faunal composition between the East Seddülbahir outcrop below the alleged MES and the main Seddülbahir section above.

Our sedimentological observations on the Gelibolu Peninsula do not show evidence of a Pliocene Gilbert delta as proposed by Melinte-Dobrinescu et al. (2009) either. In contrast, we interpret the

sedimentary successions as shoal-water delta facies. Gilbert-type deltas should show characteristic clinoform architecture that consists of steeply inclined foresets overlain by horizontal alluvial topsets and underlain by a gently inclined bottomset (Barrell, 1912; Colella, 1988; Postma, 1990). Delta topsets are expected to be prograding distributary plains where alluvial processes dominate, whereas on the coarse-grained, sandy and gravelly delta foresets gravity-driven sedimentation processes operate (Nemec, 1990). The delta deposits observed in the Gelibolu Peninsula, however, developed on shoreface sandstones as normal regressive shoreline wedges. We did not observe an erosional unconformity between the delta and the underlying shoreface sandstones and we did not find evidence of clinoformal architecture.

## 12. Conclusions

Using an integrated stratigraphic approach, we have determined the faunal assemblages and palaeoenvironments of the Seddülbahir and İntepe sections of the Dardanelles region in NW Turkey. Sedimentological analyses indicate that depositional environments are best characterised as shoal-water delta facies. Our results confirm the conventional interpretation of continuous deposition of fresh to anomalohaline/brackish water sediments during the late Miocene.

The ostracod fauna unequivocally represents middle Tortonian (late Bessarabian-Khersonian) Paratethyan assemblages. The most common mollusk species is the mactrid *Chersonimactra bulgarica*, which is also known from the middle Tortonian (Khersonian) of the Eastern Paratethys. Nannofossil assemblages show a mixing of reworked taxa. No age-diagnostic taxa have been observed. Aquatic palynological assemblages represent non-marine (fresh to oligohaline) conditions, with scarce dinoflagellates likely reworked. Radiogenic strontium ( $^{87}\text{Sr}/^{86}\text{Sr}$ ) isotope data of the anomalohaline ostracods are significantly below open ocean values and similar to values obtained from Khersonian ostracods from Eastern Paratethys deposits of Bulgaria. Fresh water assemblages reveal much higher  $^{87}\text{Sr}/^{86}\text{Sr}$  values, which are interpreted to reflect the composition of local rivers. Palaeogeographically, in late Miocene times the Dardanelles basin was a fresh to anomalohaline embayment of the Eastern Paratethys. Our re-interpretation of the Paratethys fauna and the palaeoecology and sedimentary environments of the Kirazlı-Alçıtepe formations shows a complete lack of catastrophic events and no evidence for Messinian deposits. We conclude that the presence of marine Messinian features (e.g., Messinian Erosional Surface, Zanclean flooding) in the Dardanelles region is basically a myth.

## Declaration of Competing Interest

All authors have no conflict of interest.

## Acknowledgements

This research is part of the PRIDE project (Pontocaspian Rise and DEmise), which was funded by the European Union's Horizon 2020 research and innovation program, under the Marie Skłodowska-Curie Action (grant agreement № 642973). We thank managing editor Thomas Algeo and two anonymous reviewers for their thorough and constructive comments that significantly improved the manuscript.

## Appendix A. Supplementary data

Supplementary data to this article can be found online at <https://doi.org/10.1016/j.palaeo.2020.110033>.

## References

- Alçıçek, H., Wesselingh, F.P., Alçıçek, M.C., 2015. Palaeoenvironmental evolution of the late Pliocene-early Pleistocene fluvio-deltaic sequence of the Denizli Basin (SW

- Turkey). *Palaeogeogr. Palaeoclimatol. Palaeoecol.* 437, 98–116. <https://doi.org/10.1016/j.palaeo.2015.06.019>.
- Algan, O., Çağatay, N., Tchepalyga, A., Ongan, D., Eastoe, C., Gökaşan, E., 2001. Stratigraphy of the sediment infill in Bosphorus Strait: water exchange between the Black and Mediterranean Seas during the last glacial Holocene. *Geo-Marine Lett.* 20, 209–218. <https://doi.org/10.1007/s003670000058>.
- Armijo, R., Meyer, B., Hubert, A., Barka, A., 1999. Westward propagation of the North Anatolian fault into the Northern Aegean: timing and kinematics. *Geology* 27, 267. <https://doi.org/10.1130/0091-7613>.
- Barrell, J., 1912. Criteria for the recognition of ancient delta deposits. *Bull. Geol. Soc. Am.* 23, 377–446.
- Barron, J., Badlauf, J., 1995. Cenozoic marine diatom biostratigraphy and application to paleoclimatology and paleoceanography. In: Blome, C.D. (Ed.), *Siliceous Microfossils*. 8. Paleontological Society Short Courses in Paleontology, pp. 107–118.
- Bogutskaya, N.G., Kijashko, P.V., Naseka, A.M., Orlova, M.I., 2013. Opredelitel' ryb i Bespozvonochnykh Kaspiyskogo Morya. T. 1. Ryby i Mollyuski.
- Çağatay, M.N., Görür, N., Alpar, B., Saatçılar, R., Akkök, R., Sakıncı, M., Yüce, H., Yaltrak, C., Kuşçu, İ., 1998. Geological evolution of the Gulf of Saros, NE Aegean Sea. *Geo-Mar. Lett.* 18, 1–9.
- Çağatay, M.N., Görür, N., Flecker, R., Sakıncı, M., Tünoğlu, C., Ellam, R., Krijgsman, W., Vincent, S., Dikbaş, A., 2006. Paratethyan–Mediterranean connectivity in the sea of marmara region (NW Turkey) during the Messinian. *Sediment. Geol.* 188–189, 171–187. <https://doi.org/10.1016/j.sedgeo.2006.03.004>.
- Calvert, F., Neumayr, M., 1880. Die jungen Ablagerungen am Hellespont. *Denkschriften der Kais. Akad. der Wissenschaften Math. Classe.* 40, 357–378.
- Colella, A., 1988. Pliocene–Holocene fan deltas and braid deltas in the Crati Basin, southern Italy: a consequence of varying tectonic conditions. In: Nemec, W., Steel, R.J. (Eds.), *Fan Deltas – Sedimentology and Tectonic Settings*. Blackie, London, pp. 50–74.
- Daxner-Höck, G., 1995. Some glirids and cricetids from Maramena and other Late Miocene localities in northern Greece. *Münchener Geowissenschaft. Abh. (A)* 28, 121–132.
- Delinschi, A., 2013. New dormice records (Rodentia: Gliridae) from the late Miocene of the Republic of Moldova. *Acta Zool. Cracov.* 56, 13–28.
- Di Stefano, A., Sturiale, G., 2010. Refinements of calcareous nannofossil biostratigraphy at the Miocene/Pliocene Boundary in the Mediterranean region. *Geobios* 43, 5–20. <https://doi.org/10.1016/j.geobios.2009.06.007>.
- Ercan, T., Satir, M., Steiniz, G., Dora, A., Sarıfakıoğlu, E., Adis, C., Walter, H.J., Yildirim, T., 1995. Tertiary volcanic properties Biga Peninsula, Gökceada, Bozcaada and Tavşan Islands. *Bull. Min. Res. Exp. Turkey* 117, 55–86.
- Erdogan, K., 1978. On the fossil fishes from the Tortonian of Çanakkale-Bayraktepe. *Bull. Geol. Soc. Turk.* 21, 141–144.
- Ergun, M., Ozel, E., 1995. Structural relationship between the sea of Marmara basin and the North Anatolian Fault. *Terra Nova* 7, 278–288.
- Erguvanli, K., 1955. Etude geologique de l'île de Bozcaada. *Bull. Soc. Geol. Fr.* 6, 399–401.
- Erol, O., 1992. Çanakkale yöresinin jeomorfolojisi ve neotektoniği. *Türkiye Pet. Jeologları Derneği Bülteni* 4, 147–165.
- Filippova, N.Y., Trubikhin, V.M., 2009. On the question of correlation of the Upper Miocene deposits of the Black Sea and Mediterranean basins. *Mezhdunarodnom Geolo Moscow GEOS Aktual.* 142–152.
- Frolov, P.D., Danukalova, G.A., Osipova, E.M., 2020. Late Miocene Molluscs of the Morskaya 2 Site (Azov). <https://doi.org/10.26879/936>.
- Glaubrecht, M., 1996. Evolutionsökologie und Systematik am Beispiel von Süß- und Brackwasserschnecken (Mollusca: Caenogastropoda: Cerithioidea): Ontogenese-Strategien, Paläontologische Befunde und Zoogeographie. Backhuys, Leiden.
- Glöer, P., 2019. The Freshwater Gastropods of the West-Palaeartics. Volume I. Fresh- and brackish waters except spring and subterranean snails. In: *Identification Key, Anatomy, Ecology, Distribution*. Priv. Publ.
- Gökaşan, E., Demirbağ, E., Oktay, F.Y., Ecevitoglu, B., Simsek, M., Yüce, H., 1997. On the origin of the Bosphorus. *Mar. Geol.* 140, 183–197.
- Gökaşan, E., Ergin, M., Özyalvaç, M., Sur, H.I., Tur, H., Görüm, T., Ustaömer, T., Batuk, F.G., Alp, H., Birkın, H., Türkert, A., Gezzin, E., Özturan, M., 2008. Factors controlling the morphological evolution of the Çanakkale Strait. *Geo-Mar. Lett.* 28, 107–129.
- Gökaşan, E., Görüm, T., Tur, H., Batuk, F., 2012. Morpho-tectonic evolution of the Çanakkale Basin (NW Anatolia): evidence for a recent tectonic inversion from transpression to transtension. *Geo-Mar. Lett.* 32, 227–239.
- Golovina, L.A., Radionova, E.P., Van Baak, C.G.C., Krijgsman, W., Palcu, D., 2019. A late Maeotian age (6.7–6.3 Ma) for the enigmatic “Pebbly Breccia” unit in DSDP Hole 380A of the Black Sea. *Palaeogeogr. Palaeoclimatol. Palaeoecol.* 533, 109269. <https://doi.org/10.1016/j.palaeo.2019.109269>.
- Görür, N., Çağatay, M.N., Sakıncı, M., Sümengen, M., Şentürk, K., Yaltrak, C., Tchepalyga, A., 1997. Origin of the sea of marmara from neogene to quaternary paleogeographic evolution of its frame. *Int. Geol. Rev.* 39, 342–352.
- Görür, N., Çağatay, M.N., Sakıncı, M., Tchepalyga, A., Akkök, R., Natalin, B., 2000. Neogene Paratethyan succession in Turkey and its implications for paleogeographic evolution of the Eastern Paratethys. In: Bozkurt, E., Winchester, J.A., Piper, J.A.D. (Eds.), *Tectonics and Magmatism in Turkey and Surrounding Area*. 173. Geological Society of London, Special Publication, pp. 425–443.
- Gramann, F., Kockel, F., 1969. Das Neogen im Strimonbecken (Griechisch–Ostmazedonien). Teil 1: Lithologie, Stratigraphie und Paläogeographie. *Geol. Jahrb.* 87, 445–484.
- Grothe, A., Andreotto, F., Reichart, G., Wolthers, M., Van Baak, C.G.C., Vasiliev, I., Stoica, M., Sangiorgi, F., Middelburg, J.J., Davies, G.R., Krijgsman, W., 2020. Paratethys pacing of the Messinian Salinity Crisis: Low salinity waters contributing to gypsum precipitation? *Earth Planet. Sci. Lett.* 532, 116029. <https://doi.org/10.1016/j.epsl.2019.116029>.
- Hilgen, F.J., Lourens, L.J., Van Dam, J.A., 2012. The Neogene Period. In: Gradstein, F.M., Ogg, J.G., Schmitz, M.D., Ogg, G.M. (Eds.), *The Geological Time Scale 2012*. Elsevier B.V., Amsterdam, pp. 947–1002.
- Hoernes, R., 1874. Tertiär-Studien (Teile I bis V). *Jahrb. Der k. K. Geol. Reichsanstalt* 24, 33–80.
- Hoernes, R., 1876. Ein Beitrag zur Kenntniss fossiler Binnenfaunen. (Süßwasserschichten unter den sarmatischen Ablagerungen am Marmorameere.). *Sitzungsberichte der Math. Cl. der Kais. Akad. der Wissenschaften* 74, 7–34.
- Hoyle, T.M., Leroy, S.A.G., López-Merino, L., Richards, K., 2018. Using fluorescence microscopy to discern in situ from reworked palynomorphs in dynamic depositional environments — an example from sediments of the late Miocene to early Pleistocene Caspian Sea. *Rev. Palaeobot. Palynol.* 256. <https://doi.org/10.1016/j.revpalbo.2018.05.005>.
- Ilgar, A., Sezen-Demirci, E., Demirci, Ö., 2012. Biga Yarımadası Tersiyer sedimanter istifinin stratigrafisi ve sedimantolojisi. In: Yüzer, E., Tunay, G. (Eds.), *Biga Yarımadası'nın Genel ve Ekonomik Jeolojisi*. MTA Özel Yayın Serisi, vol. 28. pp. 75–120.
- Imren, C., Le Pichon, X., Rangin, C., Demirbag, E., Ecevitoglu, B., Gorur, N., 2001. The North Anatolian fault within the Sea of Marmara: a new interpretation based on multichannel seismic and multibeam bathymetry data. *Earth Planet. Sci. Lett.* 186, 143–158.
- İslamoğlu, Y., 2009. Middle Pleistocene bivalves of the İznik lake basin (Eastern Marmara, NW Turkey) and a new paleobiogeographical approach. *Int. J. Earth Sci.* 98, 1981–1990.
- Johnson, R.A., Schofield, P.J., Williams, J.D., Austin, J.D., 2018. Salinity tolerance among three freshwater mussels (Bivalvia: Unionidae) from Gulf Coastal Plain drainages. *Florida Sci.* 81, 61–69.
- Joniak, P., de Bruijn, H., 2015. Rodents from the Upper Miocene Tuğlu Formation (Çankırı Basin, Central Anatolia, Turkey). *Paläontol. Z.* 89, 1039–1056.
- Jorissen, E.L., de Leeuw, A., van Baak, C.G.C., Mandic, O., Stoica, M., Abels, H.A., Krijgsman, W., 2018. Sedimentary architecture and depositional controls of a Pliocene river-dominated delta in the semi-isolated Dacian Basin, Black Sea. *Sediment. Geol.* 368. <https://doi.org/10.1016/j.sedgeo.2018.03.001>.
- Karakaş, Ç., Armijo, R., Lacassin, R., Suc, J.-P., Melinte-Dobrinescu, M.C., 2018. Crustal strain in the marmara pull-apart region associated with the propagation process of the North Anatolian Fault. *Tectonics* 37, 1507–1523. <https://doi.org/10.1029/2017TC004636>.
- Karakitsios, V., Cornée, J., Tsourou, T., Moissette, P., Kontakiotis, G., Agiadi, K., Manoutsoglou, E., Triantaphyllou, M., Koskeridou, E., 2017. Messinian salinity crisis record under strong freshwater input in marginal, intermediate, and deep environments. *Case North Aegean* 485, 316–335. <https://doi.org/10.1016/j.palaeo.2017.06.023>.
- Kaya, F., Kaymakçı, N., 2013. Systematics and dental microwear of the late Miocene Gliridae (Rodentia, Mammalia) from Hayranlı, Anatolia: implications for paleoecology and paleobiodiversity. *Palaeontol. Electron.* 16, 1–22.
- Kaya, T., 1982. Odontological variations of the Hippurions from Gulpinar (Canakkale). *Bull. Geol. Soc. Turk.* 25, 127–135.
- Kaya, T., 1989. Mammalian fauna of Alcitepe (Gelibolu Peninsula) surroundings: Perisodactyla findings. *Geol. Bull. Turkey* 32, 79–89.
- Koufos, G., Mayda, S., Kaya, T., 2018. New carnivore remains from the late Miocene of Turkey. *Palz* 92, 131–162.
- Krijgsman, W., Stoica, M., Vasiliev, I., Popov, V.V., 2010. Rise and fall of the Paratethys Sea during the Messinian Salinity Crisis. *Earth Planet. Sci. Lett.* 290, 183–191. <https://doi.org/10.1016/j.epsl.2009.12.020>.
- Krijgsman, W., Tesakov, A., Yanina, T., Lazarev, S., Danukalova, G., Van Baak, C.G.C., Agustí, F., Alçiçek, M.C., Aliyeva, E., Bista, D., Bruch, A., Büyükeriç, Y., Bukhsianidze, M., Kroonenberg, S.B., Lordkipanidze, D., Oms, O., Rausch, L., Singarayer, J., Stoica, M., 2019. Earth-science reviews quaternary time scales for the Pontocaspian domain: interbasinal connectivity and faunal evolution. *Earth Sci. Rev.* 188, 1–40. <https://doi.org/10.1016/j.earscirev.2018.10.013>.
- Krijgsman, W., Palcu, D.V., Andreotto, F., Stoica, M., Mandic, O., 2020. Changing seas in the late Miocene Northern Aegean: A Paratethyan approach to Mediterranean basin evolution. *Earth Sci. Rev.* in press. <https://doi.org/10.1016/j.earscirev.2020.103386>.
- Lazarev, S., 2020. From the Eastern Paratethys to the Pontocaspian basins: PhD Thesis. *Utr. Univ.* pp. 130.
- Lazarev, S., de Leeuw, A., Stoica, M., Mandic, O., van Baak, C.G.C., Vasiliev, I., Krijgsman, W., 2020. From Khersonian drying to Pontian “flooding”: late Miocene stratigraphy and palaeoenvironmental evolution of the Dacian Basin (Eastern Paratethys). *Glob. Planet. Chang.* 192, 103224. <https://doi.org/10.1016/j.gloplacha.2020.103224>.
- Le Pichon, X., Sengör, A.M.C., Demirbag, E., Rangin, C., Imren, C., Armijo, R., Görür, N., Çağatay, N., Mercier de Lepinay, B., Meyer, B., Saatçılar, R., Tok, B., 2001. The active main Marmara fault. *Earth Planet. Sci. Lett.* 192, 595–616.
- Le Pichon, X., Sengör, A.M.C., Kende, J., Imren, C., Henry, P., Grall, C., Karabulut, H., 2016. Propagation of a strike-slip plate boundary within an extensional environment: the westward propagation of the North Anatolian Fault. *Can. J. Earth Sci.* 53, 1416–1439.
- Lüttig, G., Steffens, D., 1976. Explanatory Notes for the Paleogeographic Atlas of Turkey from Oligocene to Pleistocene. Bundesanstalt für Geowissenschaften und Rohstoffe.
- McArthur, J.M., Howarth, R.J., Shields, G.A., 2012. Strontium isotope stratigraphy. *Geol. time scale* pp. 127–144. *Geol. time scale* 127–144.
- Melinte-Dobrinescu, M.C., Suc, J.-P., Clauzon, G., Popescu, S.-M., Armijo, R., Meyer, B., Biltekin, D., Çağatay, M.N., Ucaruk, G., Joannic, G., Fauquette, S., Çakır, Z., 2009. The Messinian salinity crisis in the Dardanelles region: Chronostratigraphic constraints. *Palaeogeogr. Palaeoclimatol. Palaeoecol.* 278, 24–39. <https://doi.org/10.1016/j.palaeo.2009.06.023>.



- 1016/j.palaeo.2009.04.009.
- Mudie, P.J., Marret, F., Rochon, A., Aksu, A.E., 2010. Non-pollen palynomorphs in the Black Sea corridor. *Veg. Hist. Archaeobotany* 19, 531–544.
- Nemec, W., 1990. Aspects of sediment movement on steep delta slopes. In: Colella, A., Prior, D.B. (Eds.), *Coarse-Grained Deltas*. 10. International Association of Sedimentologists, Special Publication, pp. 29–73.
- Neubauer, T.A., Harzhauser, M., Mandic, O., Georgopoulou, E., Kroh, A., 2016. Palaeobiogeography and historical biogeography of the non-marine caenogastropod family Melanopsidae. *Palaeogeogr. Palaeoclimatol. Palaeoecol.* 444, 124–143. <https://doi.org/10.1016/j.palaeo.2015.12.017>.
- Nevekskaya, L.A., Goncharova, I.A., Paramonova, N.P., Popov, S.V., Babak, E.V., Bagdasarjan, K.G., Voronina, A.A., 1993. *Opređelitel' miotsenovykh dvustvorchatykh molluskov yugo-zapadnoy Yevrazii*. Tr. Paleontol. Instituta 247, 1–412.
- Nevekskaya, L.A., Paramonova, N.P., Babak, E.V., 1997. *Opređelitel' pliotenovykh dvustvorchatykh molluskov yugo-zapadnoy Yevrazii*. Tr. Paleontol. Instituta 269, 1–267.
- Nuriel, P., Craddock, J., Kylander-Clark, A.R.C., Uysal, I.T., Karabacak, V., Dirik, R.K., Hacker, B.R., Weinberger, R., 2019. Reactivation history of the North Anatolian fault zone based on calcite age-strain analyses. *Geology* 47, 465–469. <https://doi.org/10.1130/G45727.1>.
- Okay, A., Kashişlar-Ozcan, A., Imren, C., Boztepe-Guney, A., Demirbag, E., Kuscü, I., 2000. Active faults and evolving strike-slip basins in the Marmara Sea, Northwest Turkey: a multichannel seismic reflection study. *Tectonophysics* 321, 189–218.
- Okay, A.I., Tüysüz, O., Kaya, Ş., 2004. From transpression to transtension: changes in morphology and structure around a bend on the North Anatolian Fault in the Marmara region. *Tectonophysics* 391, 259–282.
- Palcu, D.V., Popov, S.V., Golovina, L.A., Kuiper, K.F., Liu, S., Krijgsman, W., 2019a. The shutdown of an anoxic giant: magnetostratigraphic dating of the end of the Maikop Sea. *Gondwana Res.* 67, 82–100. <https://doi.org/10.1016/j.gr.2018.09.011>.
- Palcu, D.V., Vasiliev, I., Stoica, M., Krijgsman, W., 2019b. The end of the Great Khersonian Drying of Eurasia: magnetostratigraphic dating of the Maeotian transgression in the Eastern Paratethys. *Basin Res.* 31, 33–58. <https://doi.org/10.1111/bre.12307>.
- Paramonova, N.P., 1994. History of Sarmatian and Akchagyalian Bivalves. *Transactions of the Palaeontological Institute*. 260. Nauka Press, Moscow, pp. 212.
- Parke, J.R., Minshull, T.A., Anderson, G., White, R.S., McKenzie, D., Kuscü, I., Bull, J.M., Gorur, N., Sengor, A.M.C., 1999. Active faults in the Sea of Marmara, Western Turkey, imaged by seismic refraction profiles. *Terra Nova* 11, 223–227.
- Pickford, M., Mayda, S., Kaya, T., 2020. *Listriodon* Skull from the Late Middle Miocene of Nebisuyu (Çanakkale – MN 8) Turkey. *Foss. Impr.*
- Popescu, S.-M., 2006. Late Miocene and early Pliocene environments in the southwestern Black Sea region from high-resolution palynology of DSDP Site 380A (Leg 42B). *Palaeogeogr. Palaeoclimatol. Palaeoecol.* 238, 64–77. <https://doi.org/10.1016/j.palaeo.2006.03.018>.
- Popov, S.V., Nevekskaya, L.A., 2000. Late Miocene Brackish-Water Mollusks and the History of the Aegean Basin. 8. pp. 195–205.
- Popov, S.V., Shcherba, I.G., Ilyina, L.B., Nevekskaya, L.A., Paramonova, N.P., Khondkarian, S.O., Magyar, I., 2006. Late Miocene to Pliocene palaeogeography of the Paratethys and its relation to the Mediterranean. *Palaeogeogr. Palaeoclimatol. Palaeoecol.* 238, 91–106. <https://doi.org/10.1016/j.palaeo.2006.03.020>.
- Postma, G.F., 1990. An analysis of the variation in delta architecture. *Terra Nova* 2, 124–130.
- Radionova, E.P., Golovina, L.A., Filipova, N.Y., Trubikhin, V.M., Popov, S.V., Goncharova, I.A., Vernigorova, Y.V., Pinchuk, T.N., 2012. Middle-upper miocene stratigraphy of the Taman Peninsula, Eastern Paratethys. *Cent. Eur. J. Geosci.* 4, 188–204. <https://doi.org/10.2478/s13533-011-0065-8>.
- Rangin, C., Le Pichon, X., Demirbag, E., Imren, C., 2004. Strain localization in the Sea of Marmara: propagation of the North Anatolian Fault in a now inactive pull-apart. *Tectonics* 23, TC2014. <https://doi.org/10.1029/2002TC001437>.
- Rausch, L., Stoica, M., Lazarev, S., 2020. A late Miocene – early Pliocene Paratethyan type ostracod fauna from the Denizli Basin (SW Anatolia) and its paleogeographic implications. *Acta Palaeontol. Rom.* 16, 3–56.
- Rögl, F., Bernor, R.L., Dermizakis, M.D., Müller, C., Stancheva, M., 1991. On the Pontian correlation in the Aegean (Aegina Island). *Newsl. Stratigr.* 24, 137–158.
- Rückert-Ülkümen, N., Kowalke, T., Matzke-Karasz, R., Witt, W., Yigitbas, E., 2006. Biostratigraphy of the Paratethyan Neogene at Yalova (Izmit-Province, NW-Turkey). *Newsl. Stratigr.* 42, 43–68.
- Rybikina, A.I., Kern, A.N., Rostovtseva, Y.V., 2015. New evidence of the age of the lower Maeotian substage of the Eastern Paratethys based on astronomical cycles. *Sediment. Geol.* 330, 122–131. <https://doi.org/10.1016/j.sedgeo.2015.10.003>.
- Şafak, Ü., 2016. Ostracod fauna and environmental features of Tertiary (Paleogene - Neogene) deposits in Yedikule- İstanbul Region. *MTA Dergisi, Sayı 152*, 39–63.
- Şafak, Ü., Güldürek, M., 2017. Micropaleontological and Paleoenvironmental interpretations of the Boreholes from the Edirne-Kırklareli/Thrace region. *KSU. J. Eng. Sci.* 20, 90–115 (in Turkish).
- Sakıncı, M., Yaltırak, C., 2005. Messinian crisis: What happened around the northeastern Aegean? *Mar. Geol.* 221, 423–436.
- Sakıncı, M., Yaltırak, C., Oktay, F.Y., 1999. Palaeogeographical evolution of the Thrace Neogene Basin and the Tethian – Paratethian relations at Northwest Turkey (Thrace). *Palaeogeogr. Palaeoclimatol. Palaeoecol.* 153, 17–40.
- Sands, A.F., Neubauer, T.A., Nasibi, S., Harandi, M.F., Anistratenko, V.V., Wilke, T., Albrecht, C., 2019. Old lake versus young taxa: a comparative phylogeographic perspective on the evolution of Caspian Sea gastropods (Neritidae: Theodoxus). *R. Soc. Open Sci.* 6, 190965. <https://doi.org/10.1098/rsos.190965>.
- Saraç, G., 2003. Mammal Fossil Findings in Turkey. *Sci. Rep. No 10609208p*. Turkey MTA, Ankara (in Turkish).
- Şen, S., 2016. Historical background. In: Şen, S. (Ed.), *Late Miocene Mammal Locality of Küçükçekmece, European Turkey*. 38. Geodiversitas, pp. 153–173.
- Şengör, A.M.C., Tüysüz, O., İmren, C., Sakıncı, M., Eyidoğan, H., Görür, N., Le Pichon, X., Claude Rangin, C., 2005. The North Anatolian Fault. A new look. *Annu. Rev. Earth Planet. Sci.* 33, 1–75.
- Şengör, A.M.C., Grall, C., İmren, C., Le Pichon, X., Görür, N., Henry, P., Karabulut, H., Siyako, M., 2014. The geometry of the North Anatolian transform fault in the Sea of Marmara and its temporal evolution: implications for the development of intracontinental transform faults. *Can. J. Earth Sci.* 51, 222–242.
- Şentürk, K., Karaköse, C., 1987. The Geology of the Çanakkale Strait. *Sci. Rep. by Miner. Res. Explor. Dir. Turkey*.
- Sinzov, I., 1896. *Opisanie nekotorykh vidov neogenovykh okamenelostey, naydenykh v Bessarabii i v Khersonskoy gubernii*. Zap. Novorossiiskoe Obs. Estestvoispyt. 21, 39–88.
- Stancheva, M., 1972. Sarmatian Ostracodes from North-eastern Bulgaria. *Bull. Geol. Inst. Ser. Paleontol.* 21, 103–128.
- Stancheva, M., 1976. Zonation of the Sarmatian Sediments in North-eastern Bulgaria on Ostracod Fauna. *Geol. Balc.* 6, 53–59.
- Stancheva, M., 1984. Zonal subdivision of the Sarmatian Stage in North-west Bulgaria based on ostracod fauna. *Geol. Balc.* 14, 69–74.
- Stancheva, M., 1990. Upper Miocene ostracods from Northern Bulgaria. *Geol. Bulg. Ser. Operum Singul.* 5, 111.
- Stefanescu, S., 1896. Études sur les Terrains tertiaires de Roumanie. Contribution à l'étude des faunes sarmatique, pontique et levantine. *Mémoires la Société Géologique Fr. Mémoir* 15. Paléontologique 6, 1–147.
- Stevanovic, P., Nevekskaya, L.A., Marinescu, F., Sokac, A., Jámbo, A., 1989. *Chronostratigraphie Und Neostatotypen: Pliozän Pl1, Pontien. JAZU & SANU, Zagreb-Beograd*.
- Stoica, M., Lazăr, I., Vasiliev, I., Krijgsman, W., 2007. Mollusc assemblages of the Pontian and Dacian deposits from the Topolog-Argeş area (southern Carpathian foredeep – Romania). *Geobios* 40, 391–405. <https://doi.org/10.1016/j.geobios.2006.11.004>.
- Stoica, M., Lazăr, I., Krijgsman, W., Vasiliev, I., Jipa, D., Floroiu, A., 2013. Paleoenvironmental evolution of the East Carpathian foredeep during the late Miocene–early Pliocene (Dacian Basin; Romania). *Glob. Planet. Chang.* 103, 135–148. <https://doi.org/10.1016/j.gloplacha.2012.04.004>.
- Stoica, M., Krijgsman, W., Fortuin, A., Gliozzi, E., 2016. Paratethyan ostracods in the Spanish Lago-Mare: more evidence for interbasinal exchange at high Mediterranean Sea level. *Palaeogeogr. Palaeoclimatol. Palaeoecol.* 441, 854–870. <https://doi.org/10.1016/j.palaeo.2015.10.034>.
- Stoica, M., Krijgsman, W., Fortuin, A., Gliozzi, E., 2018. Reply to “Ceratolithus acutus Gartner and Bukry 1974 (= C. armatus Müller 1974), calcareous nannofossil marker of the marine flooding that terminated the Messinian salinity crisis” by Popescu et al., 2017. *Palaeogeogr. Palaeoclimatol. Palaeoecol.* 511, 646. <https://doi.org/10.1016/j.palaeo.2017.08.024>.
- Suc, J., Popescu, S., Do Couto, D., Clauzon, G., Rubino, J., Melinte-dobrincescu, M.C., Brun, J., Dumurd, N., Meyer, B., Macael, R., Tomi, D., Sokoutis, D., Rifelj, H., 2015. Marine gateway vs. fluvial stream within the Balkans from 6 to 5 Ma. *Mar. Pet. Geol.* 66, 231–245. <https://doi.org/10.1016/j.marpetgeo.2015.01.003>.
- Sümengen, M., Terlemez, İ., Şentürk, K., Karaköse, C., Erkan, E., Ünay, E., Gürbüz, M., Atalay, Z., 1987. Stratigraphy, sedimentology and tectonics of the Gelibolu peninsula and Tertiary Thrace basin. *Sci. Rep. Miner. Res. Explor. Dir. Turkey no:* 8128, 328.
- Syrides, G.E., 1998. Paratethyan mollusc faunas from the Neogene of Macedonia and Thrace, Northern Greece. *Rom. J. Stratigr.* 78, 171–180.
- ter Borgh, M., Vasiliev, I., Stoica, M., Knežević, S., Matenco, L., Krijgsman, W., Rundić, L., Cloetingh, S., 2013. The isolation of the Pannonian basin (Central Paratethys): New constraints from magnetostratigraphy and biostratigraphy. *Glob. Planet. Chang.* 103, 99–118. <https://doi.org/10.1016/j.gloplacha.2012.10.001>.
- Ternek, Z., 1949. Geological Study of the Region of Kesan-Korudag. Ph.D. Thesis. İstanbul Univ, İstanbul, pp. 78.
- Tunoğlu, C., Ünal, A., 2001a. Pannonian-Pontian ostracoda fauna of Gelibolu Neogene Basin (NW Turkey). *Yerbilimleri* 23, 167–187.
- Tunoğlu, C., Ünal, A., 2001b. Ostracoda Biostratigraphy and Chronostratigraphy of Pannonian-Pontian Sequence of Gelibolu Peninsula, NW Turkey. *Geol. Bull. Turkey* 44, 15–25.
- Umut, M., Kurt, Z., İmik, M., Özcan, L., Sarıkaya, H., Saraç, G., 1983. Tekirdağ İli-Silivri (İstanbul İli)-Pınarhisar (Kırklareli İli) Alanının Jeolojisi. *MTA Rap.* Ankara, pp. 7349.
- Ünay, E., De Bruijn, H., 1984. On some Neogene rodent assemblages from both sides of the Dardanelles, Turkey. *Newsl. Stratigr.* 13, 119–132.
- Ünay, E., De Bruijn, H., Saraç, G., 2003. A preliminary zonation of the continental Neogene of Anatolia based on rodents. In: Reumer, J.W.F., Wessels, W. (Eds.), *Distribution and Migration of Tertiary Mammals in Eurasia*. 10. Deensea, pp. 539–548.
- Van Baak, C.G.C., Radionova, E.P., Golovina, L.A., Raffi, I., Kuiper, K.F., Vasiliev, I., Krijgsman, W., 2015. Messinian events in the Black Sea. *Terra Nova* 27, 433–441. <https://doi.org/10.1111/ter.12177>.
- Van Baak, C.G.C., Radionova, E.P., Golovina, L.A., Raffi, I., Kuiper, K.F., Vasiliev, I., Krijgsman, W., 2016a. Objective utilization of data from DSDP Site 380 (Black Sea). *Terra Nova* 28. <https://doi.org/10.1111/ter.12208>.
- Van Baak, C.G.C., Stoica, M., Grothe, A., Aliyeva, E., Krijgsman, W., 2016b. Mediterranean-Paratethys connectivity during the Messinian salinity crisis: the Pontian of Azerbaijan. *Glob. Planet. Chang.* 141. <https://doi.org/10.1016/j.gloplacha.2016.04.005>.
- Van Baak, C.G.C., Krijgsman, W., Magyar, I., Sztanó, O., Golovina, L.A., Grothe, A., Hoyle, T.M., Mandic, O., Patina, I.S., Popov, S.V., Radionova, E.P., Stoica, M., Vasiliev, I., 2017. Paratethys response to the Messinian salinity crisis. *Earth Sci. Rev.* 172, 193–223. <https://doi.org/10.1016/j.earscirev.2017.07.015>.

- Vasiliev, I., Krijgsman, W., Langereis, C.G., Panaiotu, C.E., Maţenco, L., Bertotti, G., 2004. Towards an astrochronological framework for the eastern Paratethys Mio-Pliocene sedimentary sequences of the Focşani basin (Romania). *Earth Planet. Sci. Lett.* 227, 231–247. <https://doi.org/10.1016/j.epsl.2004.09.012>.
- Vasiliev, I., Iosifidi, A.G., Khramov, A.N., Krijgsman, W., Kuiper, K.F., Langereis, C.G., Popov, V.V., Stoica, M., Tomsha, V.A., Yudin, S.V., 2011. Magnetostratigraphy and radio-isotope dating of upper Miocene–lower Pliocene sedimentary successions of the Black Sea Basin (Taman Peninsula, Russia). *Palaeogeogr. Palaeoclimatol. Palaeoecol.* 310, 163–175. <https://doi.org/10.1016/j.palaeo.2011.06.022>.
- Verbrugge, L.N.H., Schipper, A.M., Huijbregts, M.A.J., Van der Velde, G., Leuven, R.S.E.W., 2012. Sensitivity of native and non-native mollusc species to changing river water temperature and salinity. *Biol. Invasions* 14, 1187–1199. <https://doi.org/10.1007/s10530-011-0148-y>.
- Welter-Schultes, F.W., 2012. European Non-marine Molluscs, a Guide for Species Identification. Planet Poster Ed, Göttingen.
- Wenz, W., 1942. Die Mollusken des Pliozäns der rumänischen Erdöl-Gebiete als Leitversteinerungen für die Aufschluß-Arbeiten. *Senckenbergiana* 24, 1–293.
- Wesselingh, F.P., Alçiçek, H., Magyar, I., 2008. A late Miocene Paratethyan mollusc fauna from the Denizli Basin (southwestern Anatolia, Turkey) and its regional palaeobiogeographic implications. *Geobios* 41, 861–879. <https://doi.org/10.1016/j.geobios.2008.07.003>.
- Wesselingh, F.P., Neubauer, T.A., Anistratenko, V.V., Vinarski, M.V., Yanina, T., ter Poorten, J.J., Kijashko, P.V., Albrecht, C., Anistratenko, O.Y., D'Hont, A., Frolov, P., Martínez Gándara, A., Gittenberger, A., Gogaladze, A., Karpinsky, M., Lattuada, M., Popa, L., Sands, A.F., van de Velde, S., Vandendorpe, J., Wilke, T., 2019. Mollusc species from the Pontocaspian region – an expert opinion list. *Zookeys* 827, 31–124. <https://doi.org/10.3897/zookeys.827.31365>.
- Witt, W., 2010. Late Miocene non-marine ostracods from the Lake Küçükçekmece region, Thrace (Turkey). *Zitteliana A* 50, 89–101.
- Yaltırak, C., Alpar, B., Sakinc, M., Yuce, H., 2000. Origin of the Strait of Canakkale (Dardanelles) Regional tectonics and the Mediterranean–Marmara incursion. *Mar. Geol.* 164, 139–156.
- Zattin, M., Okay, A.I., Cavazza, W., 2005. Fission-track evidence for late Oligocene and mid-Miocene activity along the North Anatolian Fault in south-western Thrace. *Terra Nova* 17, 95–101.